J.M. Teissier[1], I.M.L. Ridge[2] and J.M. Dodd[3] **ODN 0984**

[1]DEP Engineering, Saint Martin d'Hères, France; [2]TTI Testing, Wallingford, UK; [3]Millfield Manufacturing, Newcastle-upon-Tyne, UK

IN DEPTH ANALYSIS OF THE SOCKET TERMINATION, AND PROPOSAL FOR A NEW ROPE TERMINATION METHOD

Summary

In 1832 Guillaume Henri Dufour wrote "*it is only by friction that the cable is fixed in the socket body....*"

This paper will present results from a numerical simulation model which has been built as part of this study. The analysis shows that the socket termination works as a self-locking wedge system. The self-locking behavior is driven by the friction in the system.

The influence of each parameter (angle, length, coefficient of friction, stiffness, thickness, shrinkage, shape of the cone, initiation load, pre-stress…) has been analyzed.

The key factors related to the self-locking mechanism have been identified. The behavior of the system is very dependent of the construction and material of the rope.

The results of the analysis also show that the termination may not slide, (which may give the feeling that it is working) even if not in a self-locking situation. However, the safe use of the socket termination is limited to the self-locking configurations.

The same simulation tool has been used for the analysis of a specific socket system which has proved to be an efficient end connector for wire and fibre ropes.

The paper will also present the results of a comprehensive series of tests that have been undertaken using with this new socket system.

1 Introduction

Wherever wire or fibre ropes are used in service they must be terminated in some manner. There are many different types and designs of termination [1, 2] but all share the same purpose: they are the means of securing the end of and transmitting the working loads into the rope.

This paper focusses on the operation of one type of termination: the socket termination, which has been in use at least since the first cable suspension bridges in the 1830's. After he had built the Saint Antoine Bridge (1823), Guillaume Henri Dufour presented a description of a socket termination (Figure 1) [3]. Dufour wrote "*it is only by friction that the cable is fixed in the socket body....*".

Dufour went on to state he had also "*bent the wires down along the outer surface of the double-ended conical wedge, pressing a ring down over the outer end, and cobbled the ends of the protuberant wires*".

He goes on to say "*I stated that this was an excessive precaution as it can be shown .... But in a novel structure, it's better to err in excess than in lack of caution*".

Cette douille ABCD, de forme conique, porte deux ailes M, M, au moyen desquelles le câble peut s'attacher aux piles et aux culées. Le vide intérieur est rempli par un noyau *abcd*, qui serre les fils et les empêche de sortir. C'est uniquement le frottement qui retient le câble dans la douille; il était donc essentiel de s'assurer par une expérience préalable de la solidité de cet assemblage. C'est ce qui a été fait, et le résultat a été tout-à-fait satisfaisant.

PONTS SUSPENDUS. 117

Il est clair en effet que, pourvu que le noyau *abc* ne soit pas chassé au dehors, le câble rompra plutôt que de s'arracher. Pour empêcher tout déplacement du noyau, et comme par excès de précaution, on l'a terminé en tronc de cône *bcd*, opposé par la base au cône faisant coin *abc*; on a replié les fils sur ce tronc de cône. On les a enveloppés d'une virole BDEF, et l'on a rivé tous les fils en *mn*.

J'ai dit qu'il y avait là excès de précaution; car on peut démontrer que, si l'angle du cône *bac* n'est que double de l'angle du frottement du fer sur le fer, il faudrait une force de traction infinie dans le sens de la longueur du câble pour chasser le coin. Or, d'après ce qu'on conçoit du frottement du fer sur le fer, même avec enduit graisseux, il suffira de faire *ab* égal à cinq fois *bc* pour que le coin ne puisse pas être poussé en dehors. Nos noyaux étaient plus allongés que cela; il n'y avait donc nulle crainte à avoir; mais dans une construction nouvelle il vaut mieux pêcher par excès que par défaut de précaution.

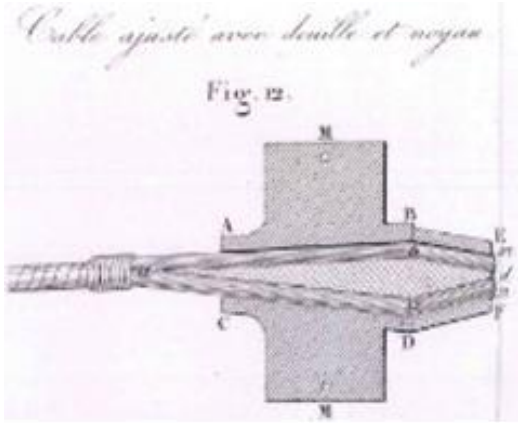

Figure 1: Extracts from Dufour's description of a socket termination in the 1830's [3].

Originally employed with wire ropes, the socketing medium, that is the material which is used to fill the conical socket, was lead or white metal [e.g. 4], but since the 1960s the use of a thermosetting resin (with filler material) was investigated as an alternative material [5, 6]. Resin is an attractive alternative to white metal as it avoids the use of molten metal and is thus safer and generally quicker to use. The use of resin as a socketing material opened up the possibility of using the socket termination for fibre ropes [7].

Analysis of sockets made employing white metal or resin as the socketing medium show that they essentially operate in the same manner [8, 9]: some initial adhesion or interaction (between rope and cone) is needed to start pulling the cone into the socket, but then as the cone is pulled down into the socket by the load in the rope, the greater the axial rope load the greater the transverse locking forces (Figure 2). There is no mechanical closure: the system works due to the increased frictional forces.

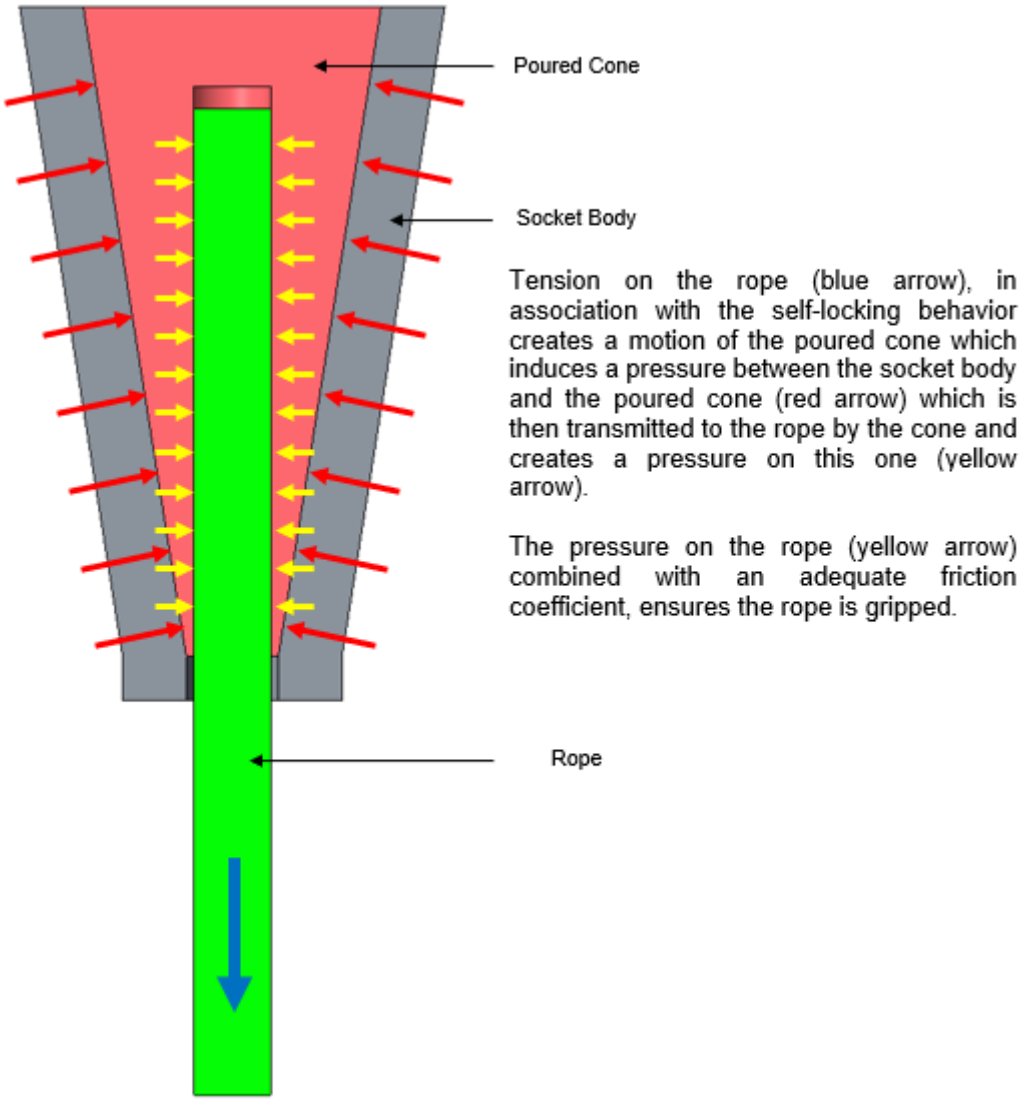

Figure 2: Principle of operation of a socket termination. (In the initial analysis the rope will be modelled as an equivalent single wire.)

The first part of this paper presents results from a numerical simulation model which was built as part of this study. The analysis shows that the socket termination works as a self-locking wedge system, and the self-locking behavior is driven by the friction in the system.

The model is used to investigate the influence of relevant parameters (cone angle, length, coefficient of friction, stiffness, thickness, shrinkage, shape of the cone, initiation load, pre-stress…).

The same simulation tool has been used to develop a novel socket system which has proved to be an efficient end connector for wire ropes and fibre.

The second part of this paper presents the results of a comprehensive series of tests that have been undertaken using with this specific new socket system.

2 The self-locking wedge system

Figure 3 presents a free body diagram of the wedge system and defines the following variables:

α :	Wedge angle
T_1 :	Friction between wedge and support
N_1 :	Action between wedge and support (normal)
T :	Friction between wedge and rope
N :	Action between wedge and rope (normal)
$\mu = \tan(\phi)$:	Friction coefficient between rope and wedge
$\mu_1 = \tan(\phi_1)$:	Friction coefficient between wedge and socket body

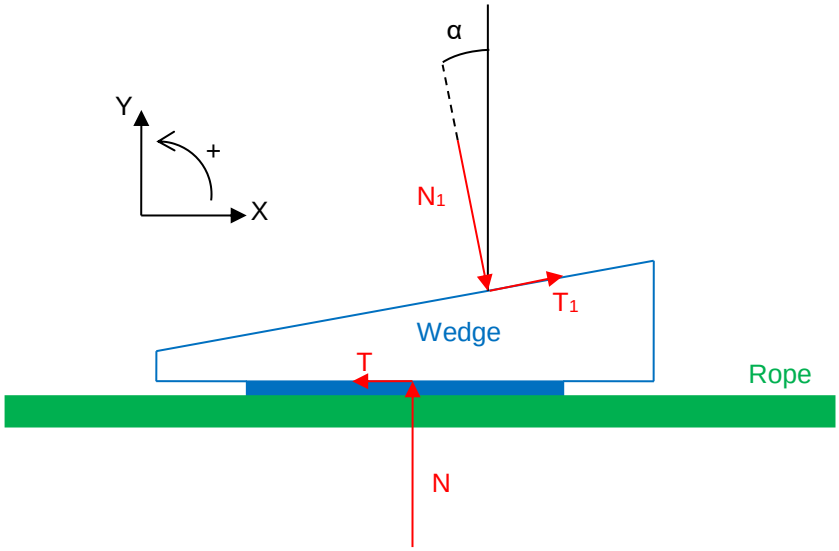

Figure 3: Definition of variables used in the analysis of a self-locking wedge system.

The equations of static equilibrium are;

X axis: $T_1.\cos(\alpha) + N_1.\sin(\alpha) - T = 0$

Y axis: $T_1.\sin(\alpha) - N_1.\cos(\alpha) + N = 0$

However, the wedge has to move, so the equations become:

$$\begin{cases} T_1.\cos(\alpha) + N_1.\sin(\alpha) - T < 0 \\ T_1.\sin(\alpha) - N_1.\cos(\alpha) + N = 0 \end{cases}$$

$$\begin{cases} T > T_1.\cos(\alpha) + N_1.\sin(\alpha) \\ N = N_1.\cos(\alpha) - T_1.\sin(\alpha) \end{cases}$$

Or $$\begin{cases} T = \mu.N \\ T_1 = \mu_1.N_1 \end{cases}$$

$$\begin{cases} \mu.N > \mu_1.N_1.\cos(\alpha) + N_1.\sin(\alpha) \\ N = N_1.\cos(\alpha) - \mu_1.N_1.\sin(\alpha) \end{cases}$$

$$\begin{cases} \mu > \dfrac{N_1.[\mu_1.\cos(\alpha) + \sin(\alpha)]}{N} \\ N = N_1.[\cos(\alpha) - \mu_1.\sin(\alpha)] \end{cases}$$

Giving the theoretical limit for the moving wedge as:

$$\mu > \frac{\mu_1.\cos(\alpha) + \sin(\alpha)}{\cos(\alpha) - \mu_1.\sin(\alpha)}$$

Table 1 below presents the results of the calculations carried out on the basis of the above formula.

alpha			friction between spelter material and socket body															
°	rd	%	0,00	0,01	0,02	0,03	0,04	0,05	0,06	0,07	0,08	0,09	0,10	0,11	0,12	0,13	0,14	0,15
0,0	0,00	0,0	0,00	0,01	0,02	0,03	0,04	0,05	0,06	0,07	0,08	0,09	0,10	0,11	0,12	0,13	0,14	0,15
0,5	0,01	0,9	0,01	0,02	0,03	0,04	0,05	0,06	0,07	0,08	0,09	0,10	0,11	0,12	0,13	0,14	0,15	0,16
1,0	0,02	1,7	0,02	0,03	0,04	0,05	0,06	0,07	0,08	0,09	0,10	0,11	0,12	0,13	0,14	0,15	0,16	0,17
1,5	0,03	2,6	0,03	0,04	0,05	0,06	0,07	0,08	0,09	0,10	0,11	0,12	0,13	0,14	0,15	0,16	0,17	0,18
2,0	0,03	3,5	0,04	0,05	0,06	0,07	0,08	0,09	0,10	0,11	0,12	0,13	0,14	0,15	0,16	0,17	0,18	0,19
2,5	0,04	4,4	0,05	0,06	0,07	0,08	0,09	0,10	0,11	0,12	0,13	0,14	0,15	0,16	0,17	0,18	0,19	0,20
3,0	0,05	5,2	0,06	0,07	0,08	0,09	0,10	0,11	0,12	0,13	0,14	0,15	0,16	0,17	0,18	0,19	0,20	0,21
3,5	0,06	6,1	0,07	0,08	0,09	0,10	0,11	0,12	0,13	0,14	0,15	0,16	0,17	0,18	0,19	0,20	0,21	0,22
4,0	0,07	7,0	0,07	0,08	0,10	0,11	0,12	0,13	0,14	0,15	0,16	0,17	0,18	0,19	0,20	0,21	0,22	0,23
4,5	0,08	7,9	0,08	0,09	0,10	0,11	0,12	0,13	0,14	0,15	0,16	0,17	0,19	0,20	0,21	0,22	0,23	0,24
5,0	0,09	8,7	0,09	0,10	0,11	0,12	0,13	0,14	0,15	0,16	0,17	0,18	0,19	0,20	0,21	0,22	0,24	0,25
5,5	0,10	9,6	0,10	0,11	0,12	0,13	0,14	0,15	0,16	0,17	0,18	0,19	0,20	0,21	0,22	0,23	0,24	0,25
6,0	0,10	10,5	0,11	0,12	0,13	0,14	0,15	0,16	0,17	0,18	0,19	0,20	0,21	0,22	0,23	0,24	0,25	0,26
6,5	0,11	11,4	0,12	0,13	0,14	0,15	0,16	0,17	0,18	0,19	0,20	0,21	0,22	0,23	0,24	0,25	0,26	0,27
7,0	0,12	12,3	0,13	0,14	0,15	0,16	0,17	0,18	0,19	0,20	0,21	0,22	0,23	0,24	0,25	0,26	0,27	0,28
7,5	0,13	13,2	0,14	0,15	0,16	0,17	0,18	0,19	0,20	0,21	0,22	0,23	0,24	0,25	0,26	0,27	0,28	0,29
8,0	0,14	14,1	0,15	0,16	0,17	0,18	0,19	0,20	0,21	0,22	0,23	0,24	0,25	0,26	0,27	0,28	0,29	0,30
8,5	0,15	14,9	0,15	0,16	0,17	0,19	0,20	0,21	0,22	0,23	0,24	0,25	0,26	0,27	0,28	0,29	0,30	0,31
9,0	0,16	15,8	0,16	0,17	0,18	0,19	0,20	0,22	0,23	0,24	0,25	0,26	0,27	0,28	0,29	0,30	0,31	0,32
9,5	0,17	16,7	0,17	0,18	0,19	0,20	0,21	0,22	0,23	0,25	0,26	0,27	0,28	0,29	0,30	0,31	0,32	0,33
10,0	0,17	17,6	0,18	0,19	0,20	0,21	0,22	0,23	0,24	0,25	0,26	0,28	0,29	0,30	0,31	0,32	0,33	0,34
10,5	0,18	18,5	0,19	0,20	0,21	0,22	0,23	0,24	0,25	0,26	0,27	0,29	0,30	0,31	0,32	0,33	0,34	0,35
11,0	0,19	19,4	0,20	0,21	0,22	0,23	0,24	0,25	0,26	0,27	0,28	0,29	0,31	0,32	0,33	0,34	0,35	0,36
11,5	0,20	20,3	0,21	0,22	0,23	0,24	0,25	0,26	0,27	0,28	0,29	0,30	0,31	0,33	0,34	0,35	0,36	0,37
12,0	0,21	21,3	0,22	0,23	0,24	0,25	0,26	0,27	0,28	0,29	0,30	0,31	0,32	0,34	0,35	0,36	0,37	0,38
12,5	0,22	22,2	0,23	0,24	0,25	0,26	0,27	0,28	0,29	0,30	0,31	0,32	0,33	0,34	0,36	0,37	0,38	0,39

Table 1: Rope-cone self-locking limit values for μ for varying values of μ_1 and α.

3 3D simulation

A 3D simulation was developed using ANSYS R16.2. Figure 4 shows the model which was modelled as a quarter of a socket since the assembly is symmetric. The model has approximately 350,000 elements.

The upper face (large diameter) of the socket was totally fixed, whilst the lateral faces had the same symmetrical constraint (Figure 4c) so they all move with their neighbour.

A force up to 250 kN was applied in 10 kN steps which permitted analysis of the results over a range of forces.

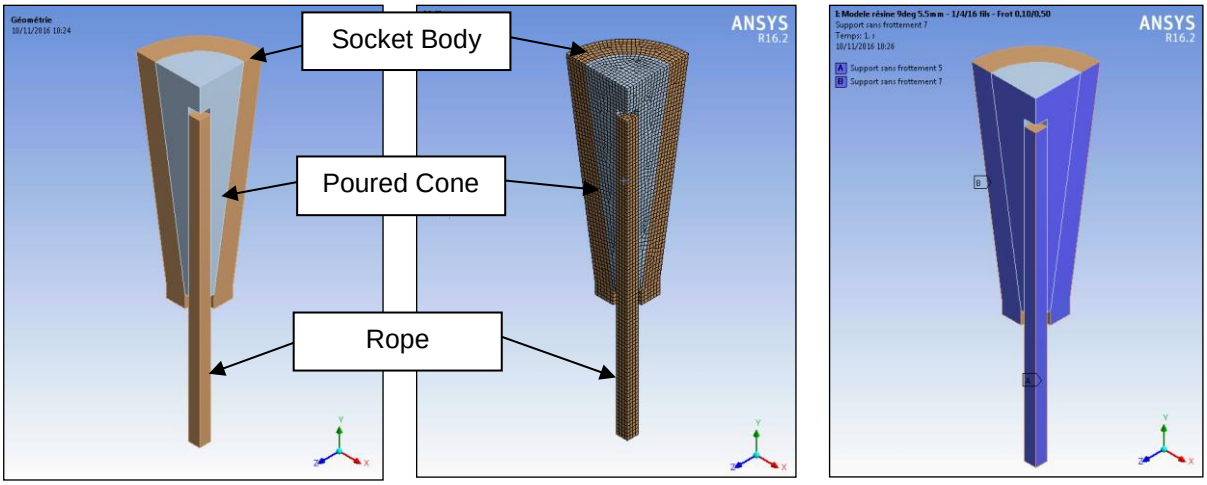

(a) model (b) finite element mesh (c) lateral face constraints

Figure 4: 3D Model of socket termination.

The model was used to explore the distribution of the load and pressure in the termination, as well as the state of contact between the rope and the poured cone (Figure 5). With reference to Figure 5c, the software gives the status of the contact:

Red = Adherence, the ratio between tangential force and normal force is lower than the friction coefficient

Orange = Sliding, the ratio between tangential force and normal force is greater than the friction coefficient

Other = No contact

In this example (Figure 5c), all the rope is in contact with the poured cone but only the bottom part is in a non-slip condition.

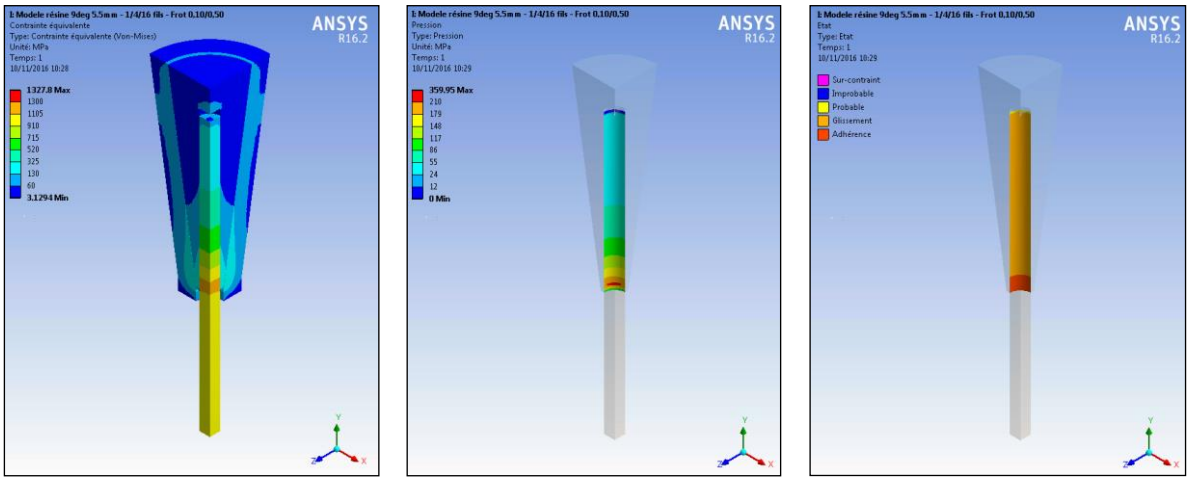

(a) stresses (b) pressure (c) contact status

Figure 5: Example stress, pressure and contact status output from the computer model.

4 Independent wedges – finite element model validation

4.1 Configuration of the validation model

As discussed above, the transmission of the load is achieved due to the compression of the poured cone. This deformation induces a loss of energy. In order to compare the results provided by the computer model with the calculations (§2), the finite element model was configured with four independent wedges (Figure 6a). Thus the efficiency (loss of energy) of the socket is not taken into consideration.

The symmetrical constraint on the lateral faces of the cone was removed (Figure 6b), so the cone effectively consists of 4 independent cones.

The friction coefficient between the poured cone and the socket body was set to 0.1, and then friction coefficient between the rope and the poured cone was adjusted until the central equivalent wire attained the non-slip state.

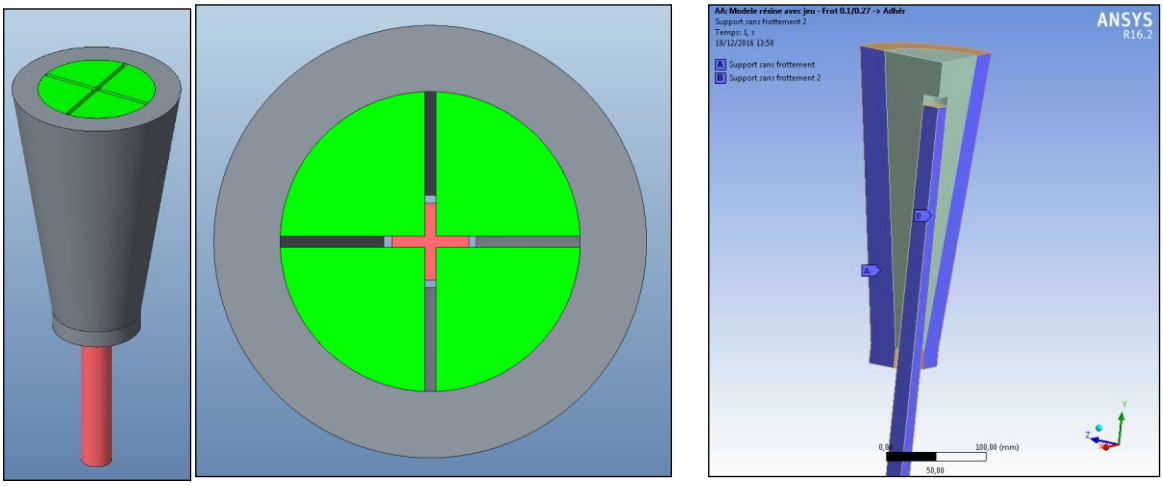

(a) Model configured with individual wedges (b) constraint removed from the cone

Figure 6: Finite element model configured as four independent wedges.

4.2 Results of the FEM validation

Figure 7 shows the results for the finite element model with the coefficient of friction between cone and socket body set to 0.1, and with a cone angle of 9°.

It can be seen that with a friction coefficient of 0.26 the non-slip status is not achieved, however, at 0.27 it is (Figure 7a).

The stress and pressure distributions are almost identical for these two values of coefficient of friction (Figure 7b and c).

Reference to Table 1 shows the calculated value of coefficient of friction $\mu = 0.27$ for $\mu_1 = 0.1$ and $\alpha = 9°$. Thus the finite element model is producing the expected results.

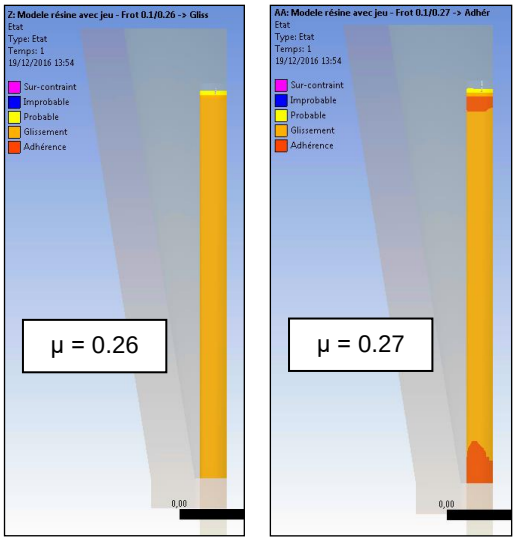

(a) non-slip state achieved with μ = 0.27

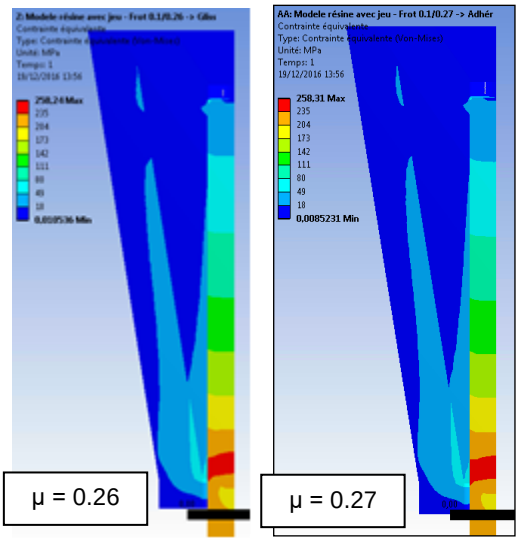

(b) stress distribution

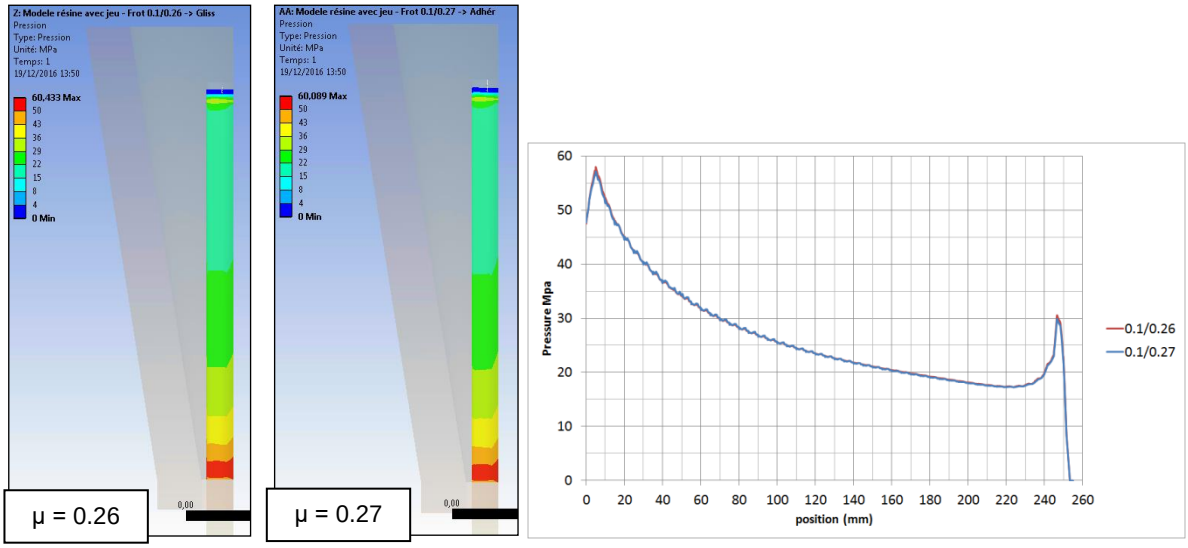

(c) pressure distribution

Figure 7: Finite element model results with $\mu_1 = 0.1$ and $\alpha = 9°$ for $\mu = 0.26$ and 0.27.

5 Functioning of a socket termination

5.1 Modelling initiation – seating of the cone

In order to start generating the wedge gripping forces, an initial force has to pull the poured cone into the socket so that all the parts are in contact.

This force, even if it is very light, creates an initial pressure on the rope, which with the frictional coefficient creates a resistance force. The chain reaction is initiated.

This initial force can be generated by many ways:

- Mechanical closure (hooking of some wires)
- Adhesion between the components
- Pre-stress of the cone

5.2 Modelling of seating of the cone

For the FEM simulation, we have again used a quarter model because the problem is symmetric. Also as before, the socket has an angle of 9°. In this example, the poured cone is made out of resin. A tension is applied to the end of the rope. To simulate this force the rope is attached to the poured cone by a spring (Figure 8).

With reference to Figure 8, just for the purposes of demonstration a small gap has been created between the wire and the hole in the poured cone. At the beginning of the simulation the tension applied to the rope is transmitted to the poured cone by the spring. The cone is then pushed against the socket body.

While moving forward the cone is compressed against the socket body and then the “artificial” gap is compensated.

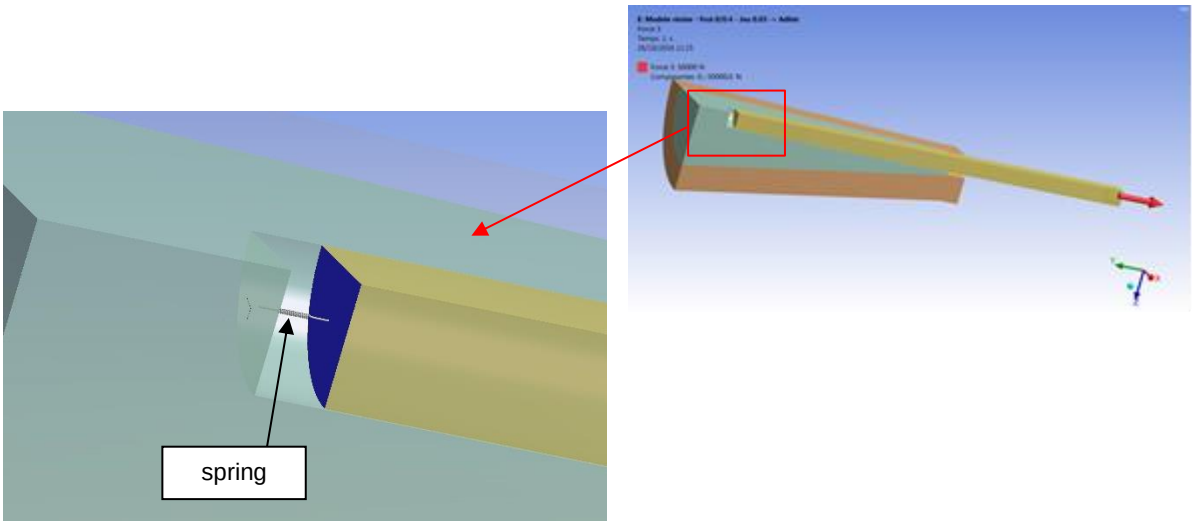

Figure 8: Simulation of initiation force in the FE model by means of a spring.

Until the spring force reaches 5% of the maximum load, there is almost no force transferred by friction, because the compression of the cone is not sufficient to compensate the “artificial” initial gap (Figure 9).

From this point a pressure is applied on the rope which initiates a resistance force, due to the friction. From then an increasing part of the tension is transmitted by the friction.

Without the initial force created by the spring, the rope would just slide in the poured cone. The force in the spring is called the “initiation” force.

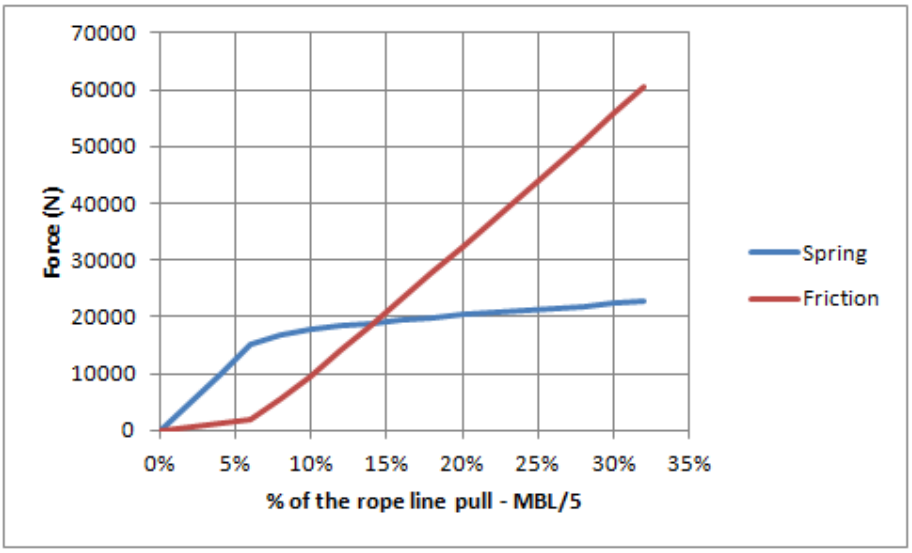

Figure 9: Showing the initiation force required in the "spring" to initiate the friction gripping of the rope in the (resin) socket cone.

5.3 Mechanical closure (hooking of some wires)

As mentioned above, the initiation force may be generated by (e.g.) hooking wires in the socket. If the system is in the self-locking configuration (the hooked wires pull the cone into the socket to generate the friction gripping) it may be seen that the hooked and the non-hooked wires take the same share of the load (Figure 10).

If cone does not seat, then the system is *not* in the self-locking configuration, and only the hooked wires are supporting the load (Figure 11) (see also §7.1).

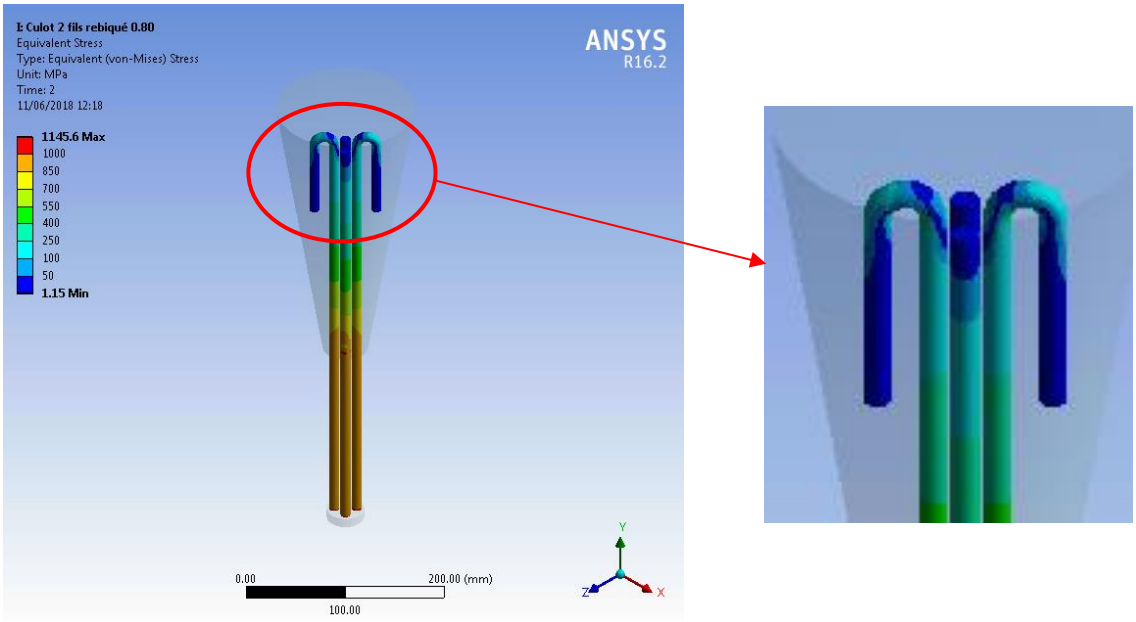

Figure 10: Even load sharing between hooked and non-hooked wires in a self-locking configuration.

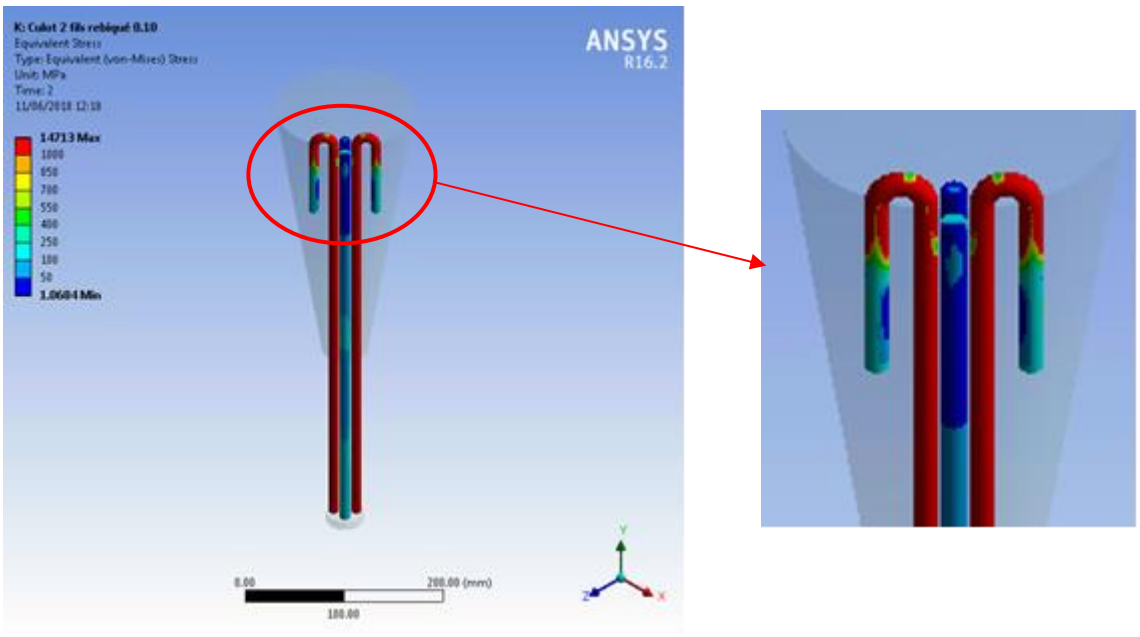

Figure 11: Un-even load sharing between hooked and non-hooked wires in a non-self-locking configuration.

5.4 Adhesion between the wires and the poured cone

Adhesion (the gluing force) may provide the force required for the initiation of the self-locking mechanism.

We can assume that the resin socket may correspond to this situation. This is not the case for metal socketing (VG3 or equivalent) especially with non-galvanized wires.

5.5 Pre-stress of the cone

In this scenario, the initiation is provided by an external means, thanks to a force introduced in the system. The simulation model converges only if such force is applied.

For all the calculations, when the system does not include a specific initiation (hooked wire, spring), a force of about 1% of the final pulling force is applied to the cone (Figure 12).

The pre-stressing is an efficient process for ensuring the initiation of the self-locking process.

It can however be misleading, and convert a non-self-locking configuration into a self-locking one, as shown in the simulation below.

The conditions for the model are:

- one wire
- 9° resin poured cone
- 50% of diameter rope for thickness of resin (see §6.6)
- friction coefficient of 0.15 between poured cone and the socket body

For this configuration the self-locking conditions are fulfilled with a friction coefficient (wire/poured cone) from 0.76 upwards. The following simulation uses a friction coefficient of 0.75.

A force of 50 kN is applied to the poured cone, which represents 20% of the total force that will be applied on the wire.

The results show that the pressure on the wire is higher with the pre-loading (Figure 13).

For the same configuration (μ_1 = 0.15 / μ = 0.75), the socket is ok with pre-stress and it slides without pre-stress (Figure 14). That is still the case with the frictional coefficients 0.15 / 0.70.

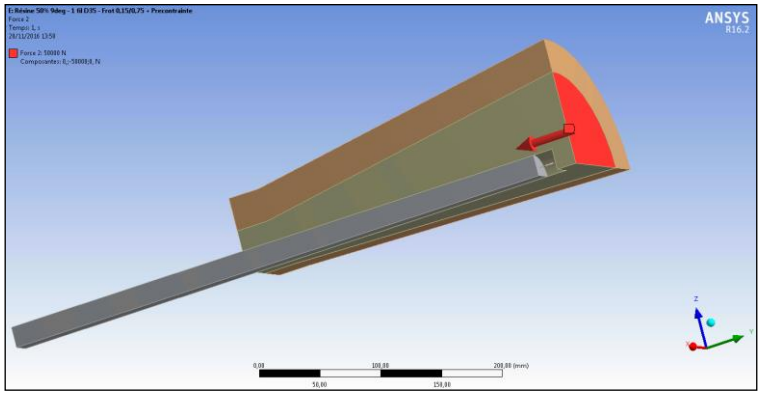

Figure 12: Application of external initiation load.

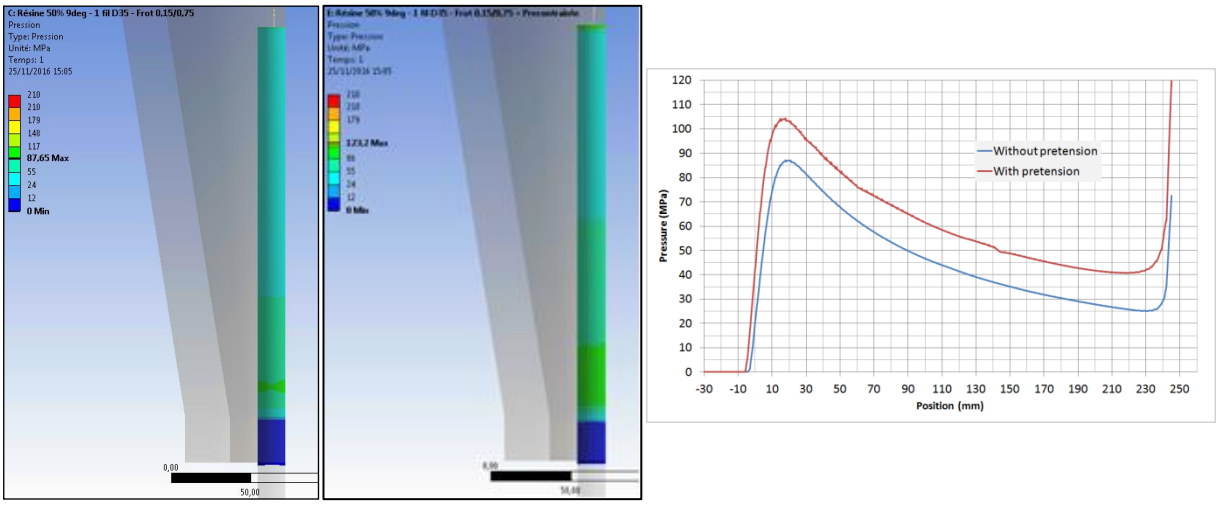

(a) non-pre-loaded cone (b) pre-loaded cone (c) pressure distribution along the cone

Figure 13: Comparison of pressure distribution in the wire with and without cone pre-load.

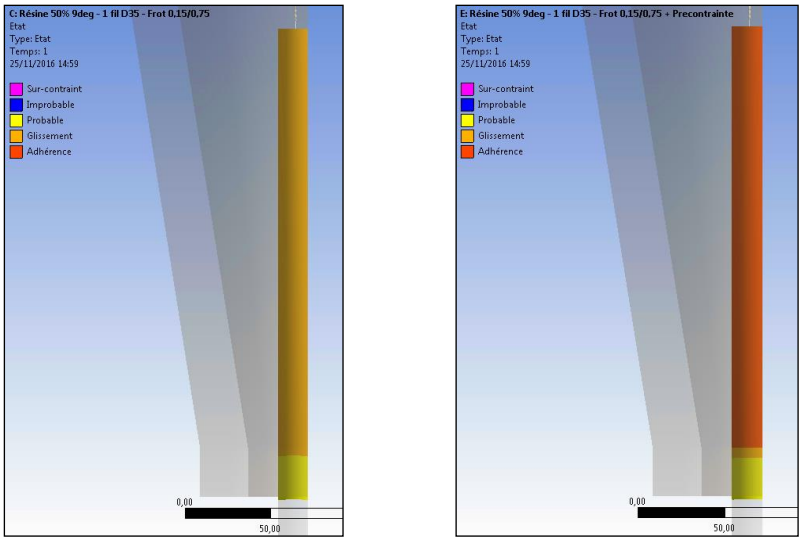

(a) no pre-stress (b) with pre-stress

Figure 14: Comparison of the wire status without and with cone pre-stress. (The wire slides without pre-stress for the given parameters.)

6 Analysis of the main parameters

This section investigates the effect of variation of various parameters on the socket operation. These include:

- The stiffness of the materials
- The shrinkage of the poured (cone) material
- The geometry (angle, length, shape) of the cone
- The "thickness" of the poured cone
- The frictional coefficient between the socket body and the poured cone, μ_1
- The frictional coefficient between rope/fibre/wire and the poured cone, μ

6.1 Stiffness of the materials

The fabrication (socketing medium) of a socket can be made with different kinds of material usually, metallic alloy or resin. The main difference between these materials is the Young's modulus:

- Steel (socket body): 210 000 MPa
- Zinc alloy (VG3): 30 000 MPa
- Resin (Wirelock): 8 000 MPa
- Wire radial stiffness: variable

For these simulations, the socket is 9° and a thickness of poured cone of 15% of the rope diameter (see §6.6).

With the same wire/fibre the status of adherence requires a higher friction coefficient if the stiffness of the poured material increases.

Considering an ideal friction coefficient between the poured cone and the socket body of zero ($\mu_1 = 0$), the adherence status requires:

- VG3 (metallic alloy), a friction coefficient with the wire/fibre of 0.29.

- Resin (Wirelock), a friction coefficient with the wire/fibre of 0.23.

With the same cone material, the status of adherence worsens if the radial stiffness of wire decreases. The same configuration is used for each model below (Figure 15):

- Socket angle 9°
- Friction coefficient between poured cone and its support is 0.15
- Friction coefficient between poured cone and rope is 0.60
- 15% of the rope diameter for the resin thickness at the bottom
- Radial stiffness of the wire, variable: 200,000 MPa – 25,000 MPa
- Poisson's ratio of resin taken as 0.35

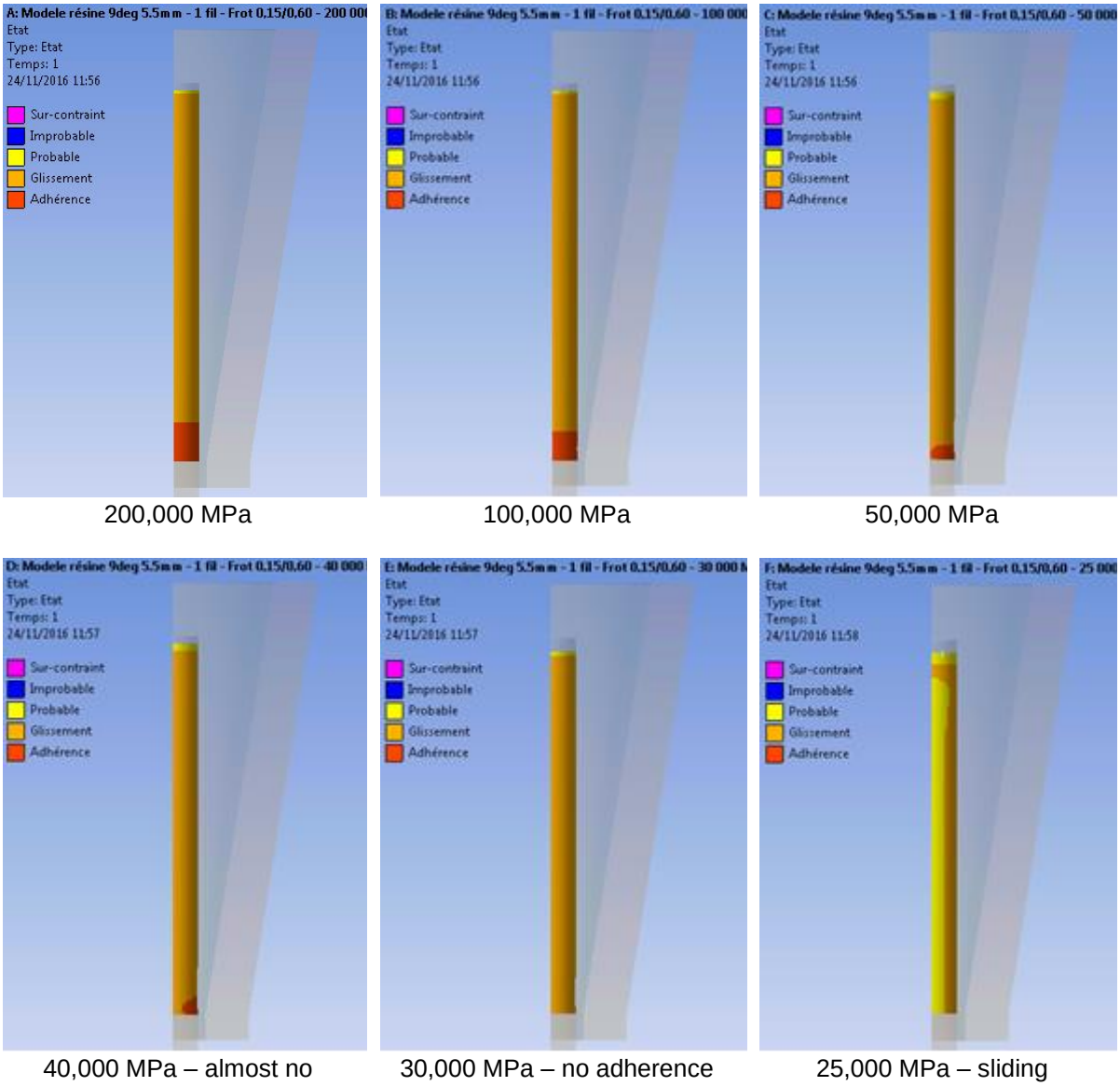

200,000 MPa | 100,000 MPa | 50,000 MPa

40,000 MPa – almost no adherence | 30,000 MPa – no adherence | 25,000 MPa – sliding

Figure 15: Effect of radial stiffness of the wire on the adherence between socket cone and wire.

The decrease in the stiffness of the wire/fibre leads irreparably to a reduction of the adhesion capability.

The significant parameter is the relative stiffness between these three elements: socket body, poured cone, and wire/fibre.

Turning to consider the pressure one the wire, the decrease in the stiffness of the wire/fibre leads to a reduction of the pressure.

It is noted that the maximum pressure remains almost steady until 40 000 MPa and then decreases rapidly (Figure 16). The reason for this behavior (in this example) relates to the relative stiffness of the wire and resin cone. So long as the wire is stiffer than the cone, forces can be transmitted. As soon as the cone is stiffer than the wire, the cone cannot be compressed enough to compress the wire. The behavior changes dramatically (30,000 MPa and 25,000 MPa) as the system get close to the limit.

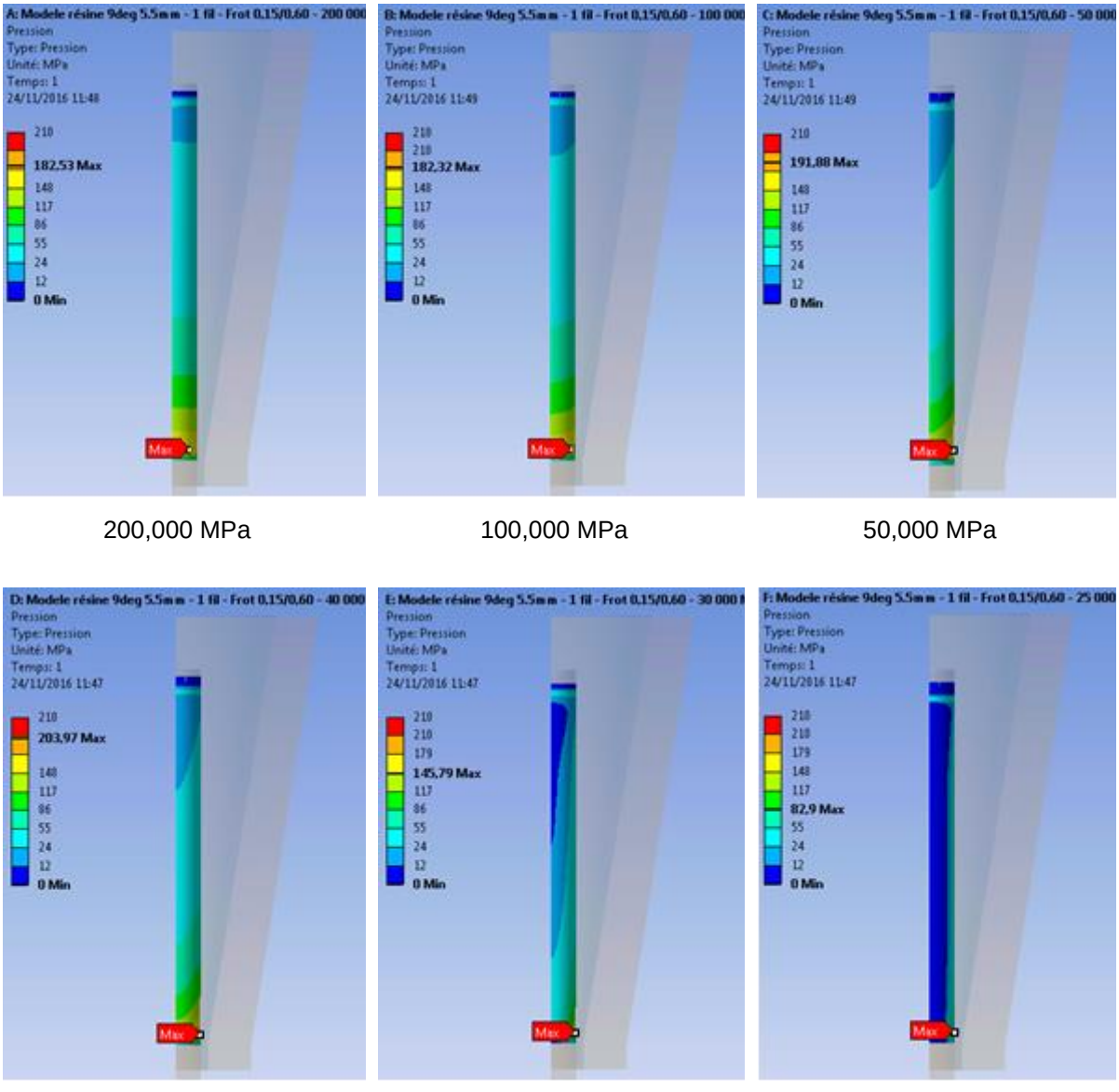

200,000 MPa | 100,000 MPa | 50,000 MPa

40,000 MPa | 30,000 MPa | 25,000 MPa

Figure 16: Effect of radial stiffness of the wire on the pressure distribution in the wire (for Resin cone, Young's Modulus 8,000 MPa).

6.2 Shrinkage of the poured material

Owing to the shrinkage of the poured material the “internal” cone (poured material), and the “external” cone (socket basket) will not have the same angle.

The shrinkage ratio of the resin is about 2%. However, the cone is not only made out of poured material, but also of steel wire / fibre.

Thus we have performed calculations for the following shrinkage ratio; 0%, 0.5%, 1% and 2%.

Figure 17 shows the pressure between the two cones (socket body and poured material) for the range of shrinkage ratios.

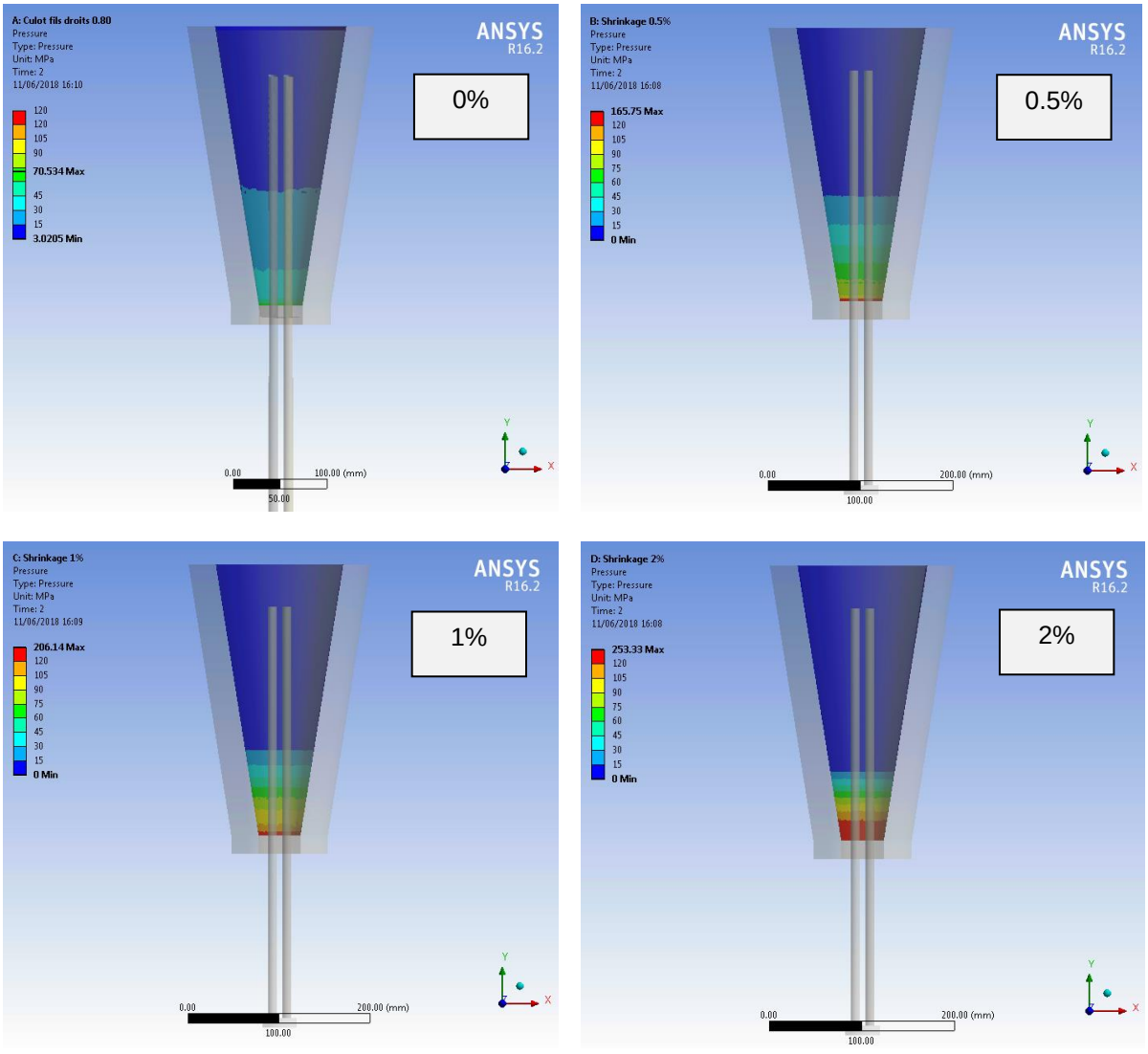

Figure 17: Pressure distribution in poured cone for a range of shrinkage ratios.

We notice that the pressure increases significantly when the shrinkage ratio increases (Figure 18). Compared to the theoretical ideal material with no shrinkage, it can be seen that the actual pressure is a factor of 2.5 or 3 greater.

Furthermore not only the intensity of the pressure is significant but also the percentage of the loaded zone. Here again the influence of the increase of the shrinkage is tremendous.

The calculations with shrinkage are much longer than without shrinkage (the condition of contact requires a lot of iterations before becoming stable). Thus all the calculations for the analysis of the parameters will be performed without shrinkage.

shrinkage	pressure	
ratio	Mpa	
0,0%	70,53	100%
0,5%	165,75	235%
1,0%	206,14	292%
2,0%	253,33	359%

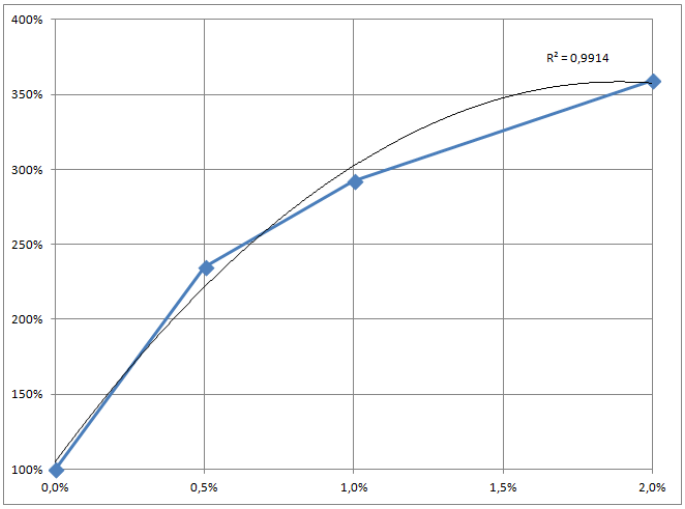

Figure 18: Effect of shrinkage ratio on maximum pressure.

6.3 Angle of the poured cone

For this comparison, we will consider:

- socket body angles α = 4°, 6°, 9° and 12°.
- The cone is made out of resin.
- The frictional coefficient between poured cone and support is 0,1; and,
- the frictional coefficient between wire/fibre rope (equivalent wire) and poured cone is 0.7.

With these conditions all socket bodies are in the self-locking condition. A force of 250 kN is applied to the lower face of the equivalent wire.

Figure 19 shows the results of this analysis. There is a stress concentration at the end of poured cone. The “nominal” stress in the “equivalent wire” is about 1,040 MPa but at the end of the poured cone the stress is over 1,200 MPa.

This overstress is almost the same for each case. But for the smallest angle, this overstress is general, while for biggest angle, the overstress is just located on the surface.

Pressure behaves similarly to the stresses. The “peak” pressure is almost the same in each case. But for the smallest angle, this high pressure is general, while for biggest angle, the overstress is just localized (Figure 20).

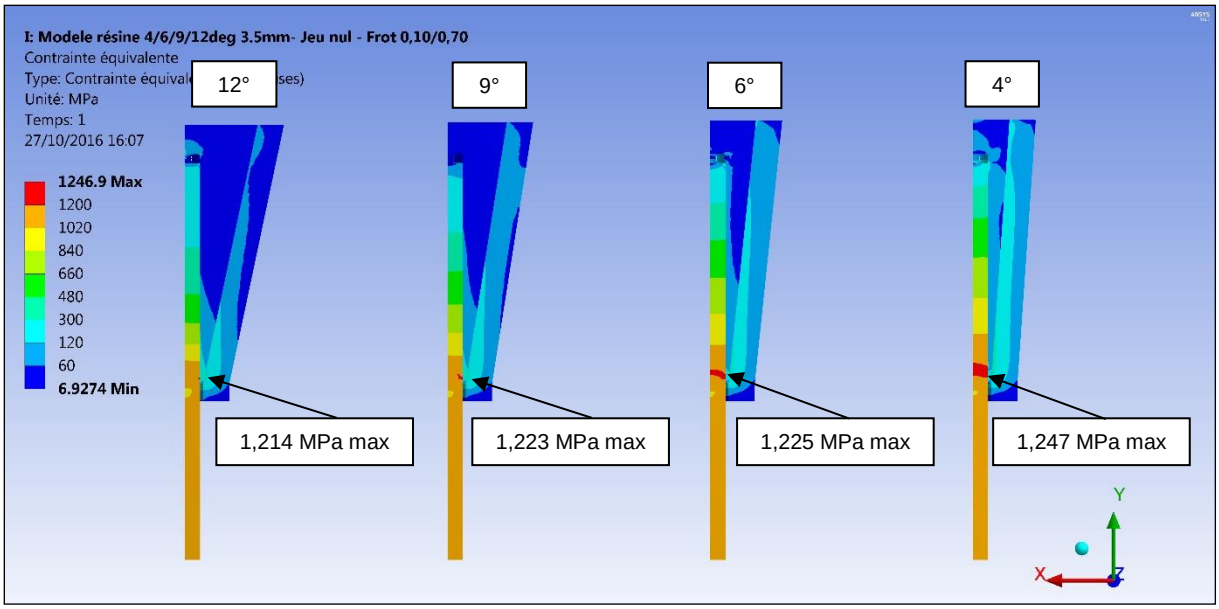

Figure 19: Distribution of stress in the socket with varying poured cone angle.

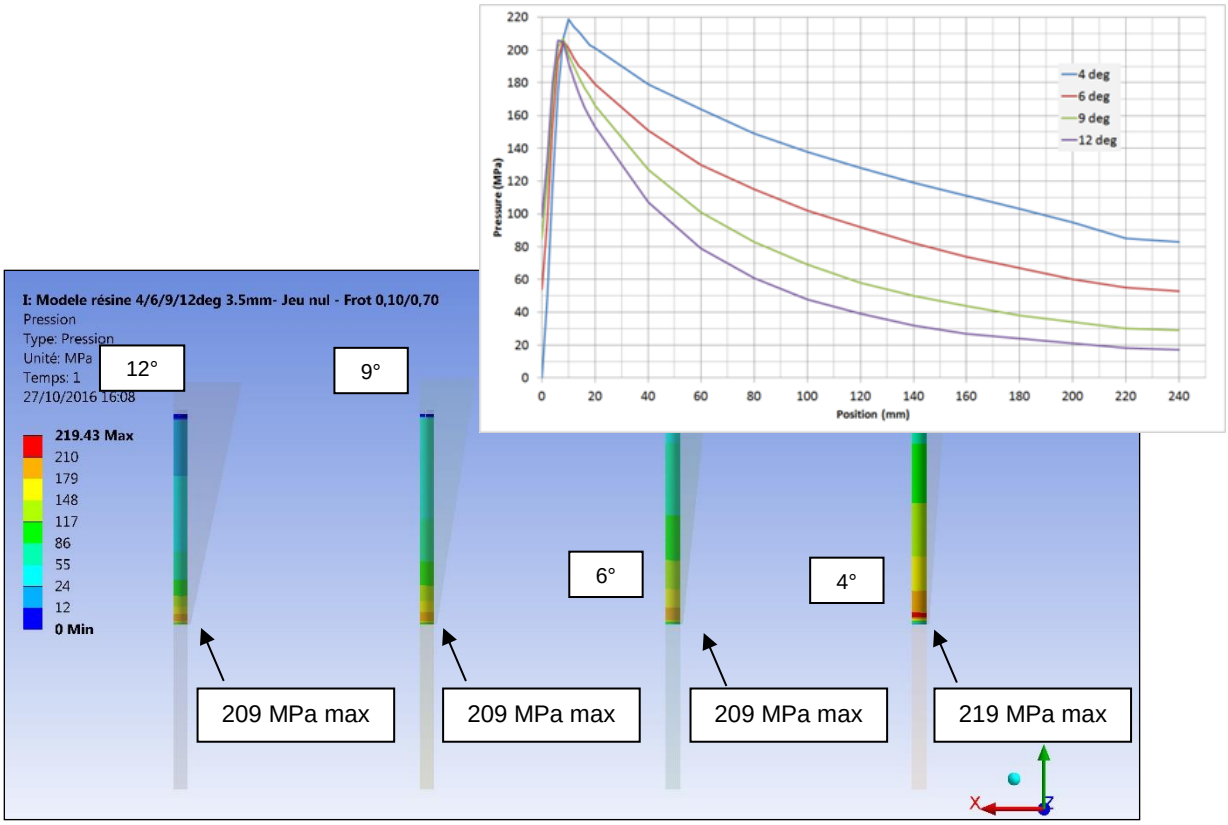

Figure 20: Distribution of pressure on the wire for varying cone angles.

For the same frictional coefficients, a socket termination with a smaller angle has a better adherence (Figure 21), but the stresses are higher in the “equivalent wire”.

The more interesting configuration is the 9 degrees. There is no big stress concentration at the bottom, a good adherence and a good distribution of the pressure.

The next analysis will mainly be carried out with a poured cone of 9°.

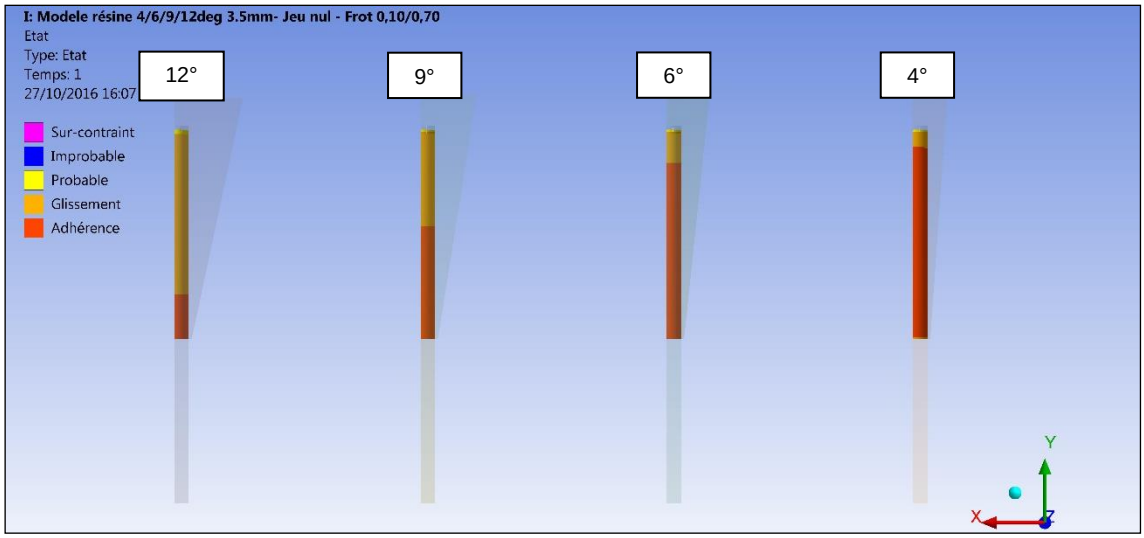

Figure 21: Variation in adherence between the cone and the wire for varying cone angles.

6.4 Length of poured cone

So far the analysis seems to indicte that the top of the socket termination is not used much. So the same configuration was tested in different sizes:

- 9° poured cone
- 50% of diameter rope for thickness of resin (see § 7.6)
- 0.15 friction coefficient between poured cone and the socket body
- 0.80 friction coefficient between poured cone and wire/fibre
- 280 mm, 210 mm and 140 mm are the lengths/heights of socket

The stress (Figure 22) has the same behavior as the pressure (Figure 23). The shorter the socket, the higher the stress/pressure. With the “long” socket it might be tempting to think that the top part of the socket, with the low stress level is useless. This would be a mistake, the suppression of this zone leads to a tremendous increase of the stress in the bottom part of the socket. In all three cases there is adherence (Figure 24).

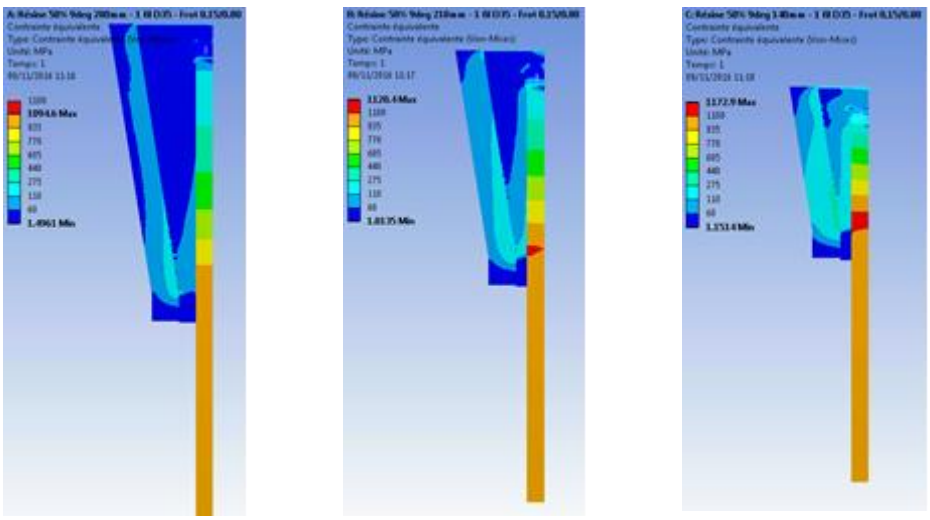

Figure 22: Variation in stress distribution for different cone lengths (280 mm, 210 mm and 140 mm).

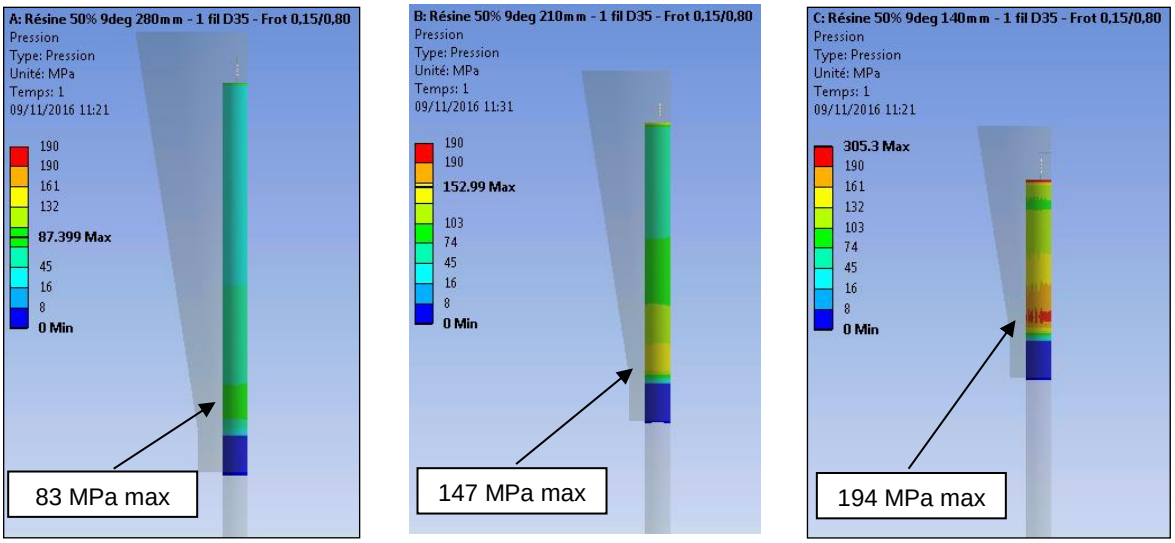

Figure 23: Variation in pressure acting on the wire for different cone lengths.

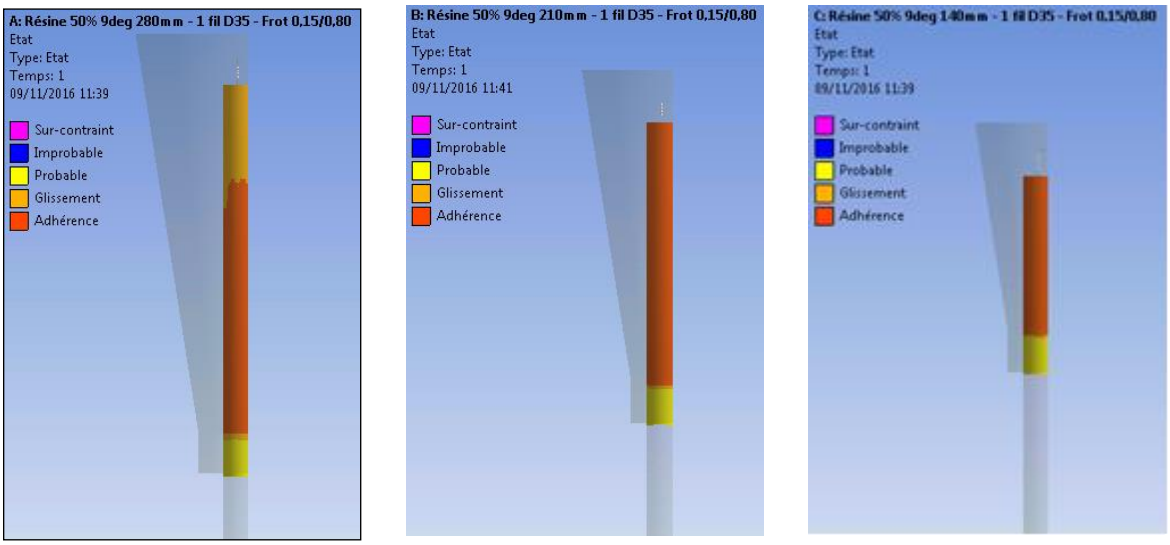

Figure 24: Variation in adherence between the cone and the wire for different cone lengths.

6.5 The shape of the cone

Three different shapes of cone have been considered (Figure 25): tulip, cone and lys. It is noted that the “initiation” force is bigger for the non “straight” shapes (Table 2).

	Tulip	Conical	Lys
	kN	kN	kN
Friction / Self-locking	215 588	243 210	238 240
Spring / Inititaion	34 412	6 790	11 760
Total	250 000	250 000	250 000
Initiation	13,8%	2,7%	4,7%

Table 2: Summary of the required initiation force required for the different cone profiles studied.

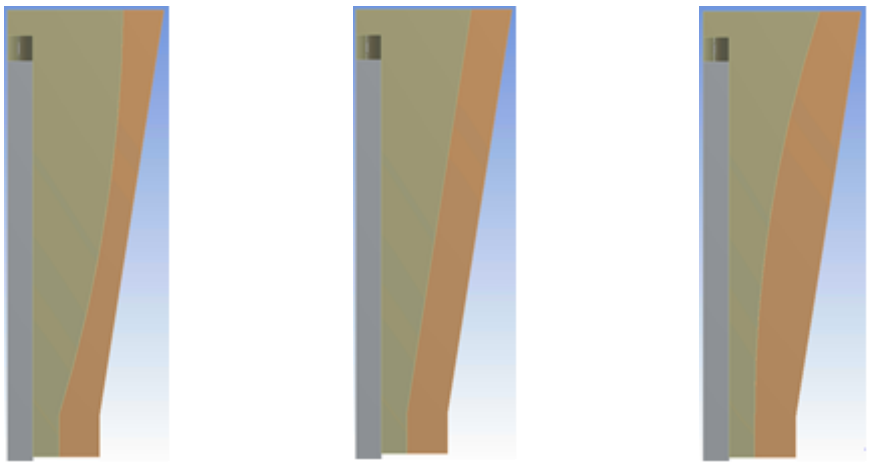

(a) tulip (b) cone (c) lys

Figure 25: Different cone profiles studied.

Turning to the pressure distribution (Figure 26), it may be seen that the tulip shape is the worst, having a higher pressure over a significant area.

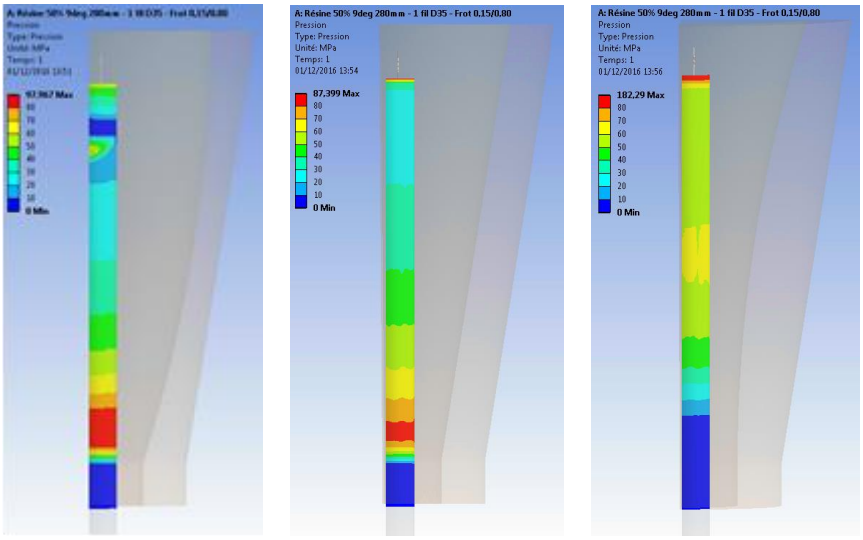

(a) tulip (b) cone (c) lys

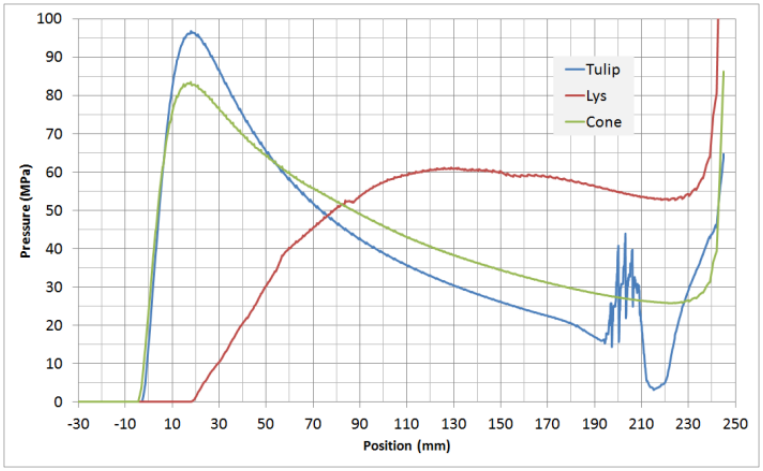

(d) pressure distribution along the socket length

Figure 26: Comparison of the pressure distribution in the different cone profiles studied.

The conical shape also provides the larger zone with the proper adhesion status (Figure 27).

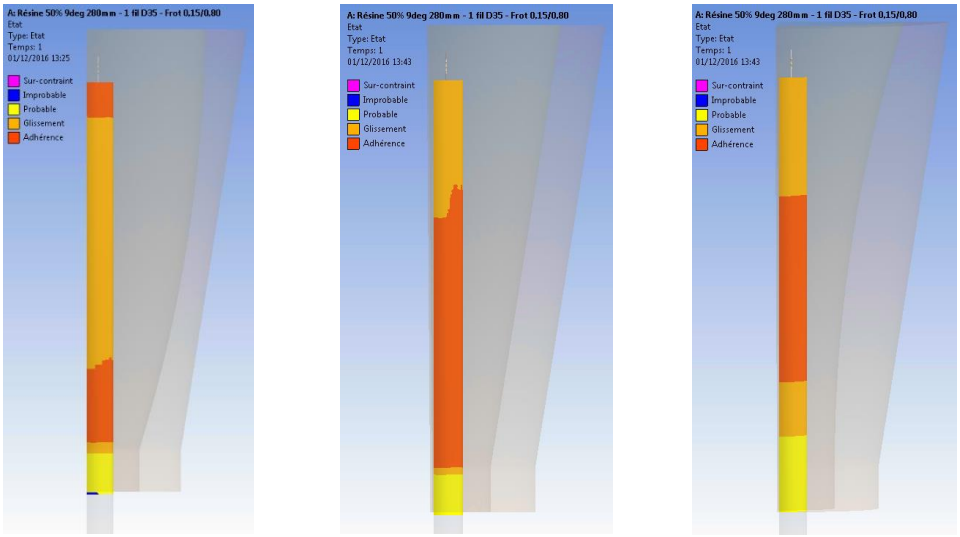

(a) tulip (b) cone (c) lys

Figure 27: Comparison of adhesion status for the different cone profiles studied.

6.6 Thickness of the poured cone

With classical socket terminations, one of the critical points is located at the “bottom”, that is where the rope exits the termination. In this position the stress concentration can act to reduce the “wire/fibre rope” strength.

A good socket termination has to reduce this stress concentration in order to reduce the effect on the “wire/fibre rope” strength and thus increase the efficiency of the termination.

This section presents an analysis of effect of variation of the ratio between the wire and the diameter of the socket exit hole. After many tests with the thickness (Figure 28) of the resin, it was found that a bigger thickness of resin is better for the “equivalent wire”.

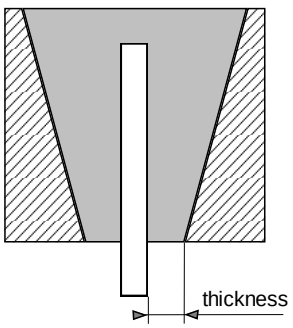

Figure 28: Definition of the term “thickness.

The same configuration was tested in different thicknesses:

- 9° poured cone
- 0.10 friction coefficient between poured cone and the socket body
- 0.56 friction coefficient between poured cone and wire/fibre
- Thickness of 15%, 30% and 50% of the “equivalent wire” diameter

As already seen for other parameters, the peak stress is almost the same for the three models, but as the thickness decreases, the area experiencing the peak stress grows and is not so localized (Figure 29). The increase of the thickness reduces significantly the pressure (Figure 30).

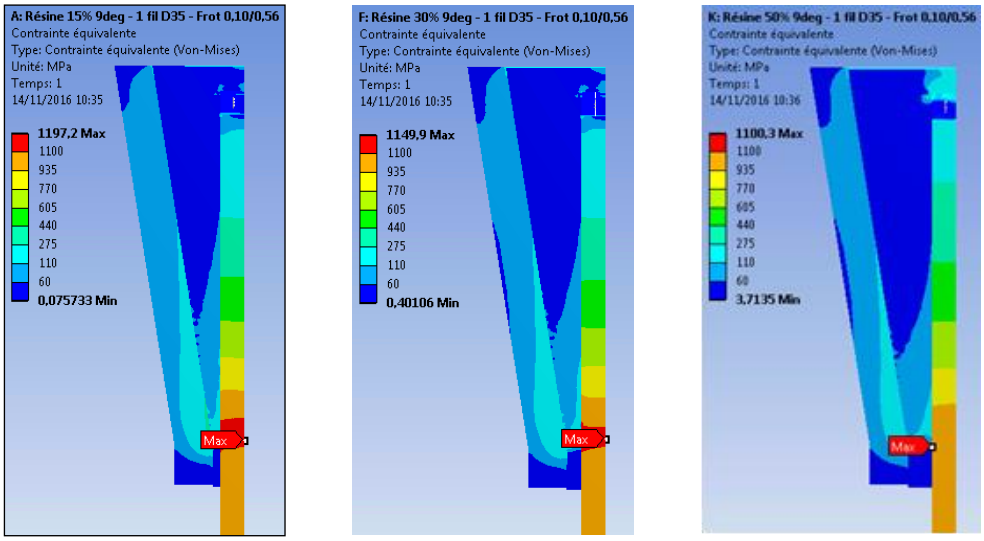

(a) 15% (b) 30% (c) 50%

Figure 29: Comparison of stress distribution for the different cone thicknesses.

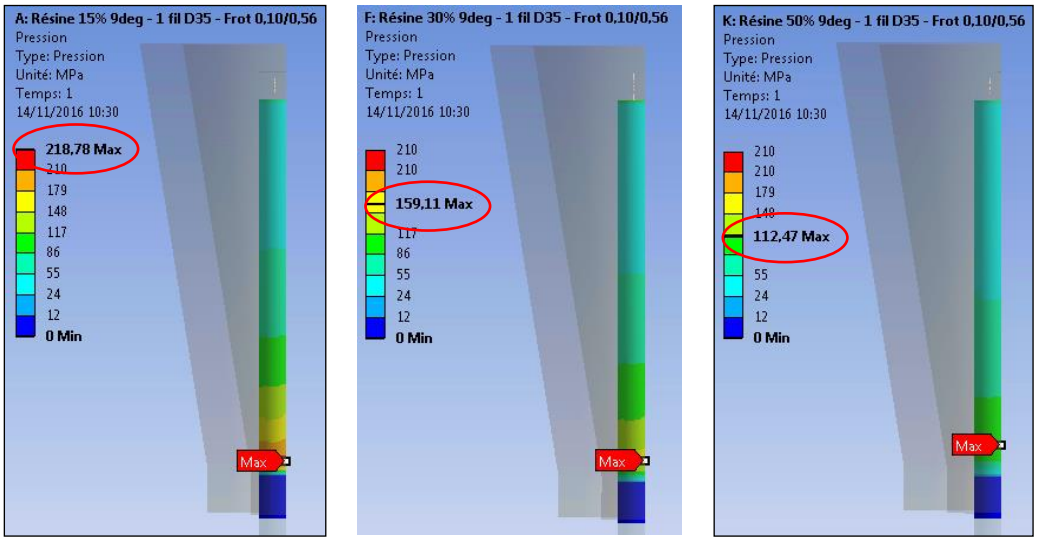

(a) 15% (b) 30% (c) 50%

Figure 30: Comparison of pressure distribution for the different cone thicknesses.

Figure 31 shows how the length of the zone with “adherence” status, reduces with increasing thickness. This is not surprising, and there will be a limit beyond which it is not beneficial to increase the thickness. The 50% thickness however, provides a sufficient length with the proper status.

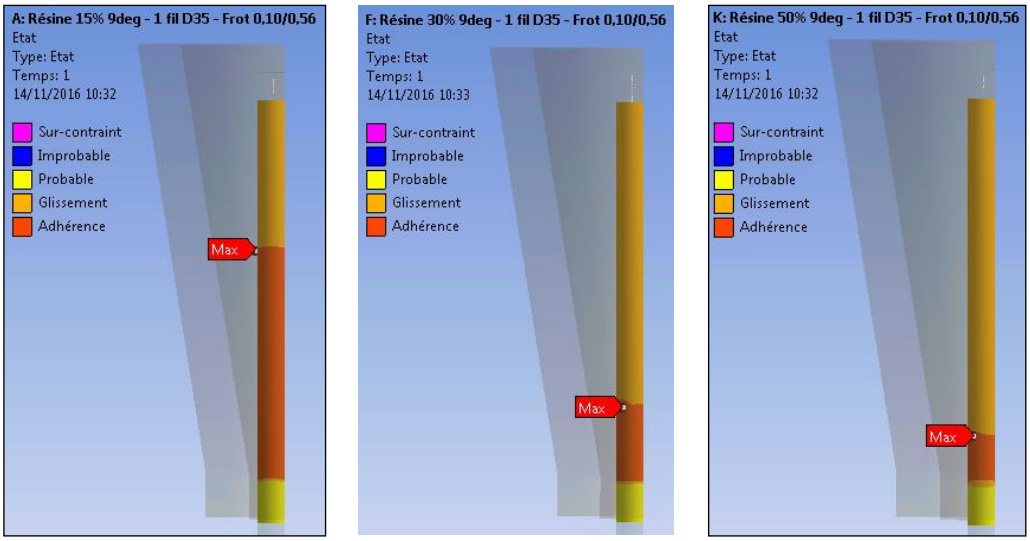

(a) 15% (b) 30% (c) 50%

Figure 31: Comparison of adherence status for the different cone thicknesses.

As a final comment, it is noted that letting the poured material move into the cylindrical base of a socket is a good option (Figure 32). It helps to spread the areas of the maximum of pressure and the stress due to the torque or other mechanical movement.

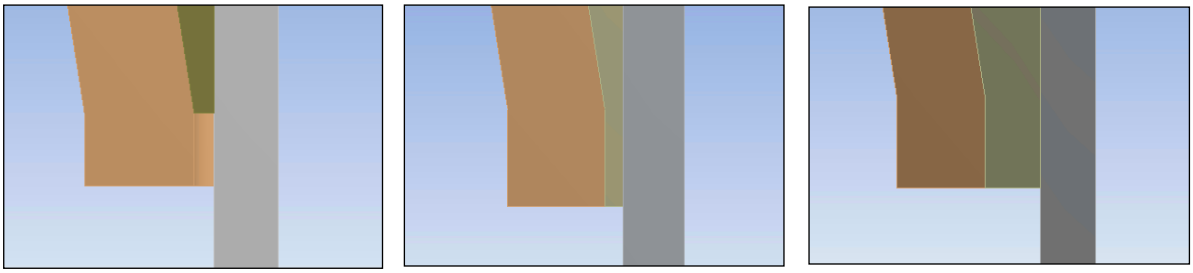

(a) initial configuration (b) better configuraion (c) best configuration

Figure 32: Configurations of cylindrical socketing medium in poured cones.

7 A note of caution – false conical sockets

7.1 Non-self-locking arrangement

A false conical socket looks like a real socket and may also behave like a real socket.

However, if the system does not fulfill the self-locking conditions, then the forces are transferred by the hooked wires. The following simulations had thus to consider hooked

wires, because without this arrangement the wires will slip and the model does not converge.

Stresses in the hook of the wire increase almost proportionally with the line pull. As the line pull decreases the stresses do the same… which leads to fatigue loading along the wire in the cone.

For the friction coefficient of 0.10 (Figure 33a), the stress in the wires remains the same as at the entrance in the socket, so all the forces are transferred via the hooks which are then overloaded.

For the friction coefficient of 0.40 (Figure 33b), which is still a non-self-locking configuration, it can be seen that the pushing force provided by the hooks of the wire, make it possible to get a part of the load supported by friction on the bottom part of the wire. So, the hooking of the wires can give the feeling that the socket is working properly, but in fact the force is only supported by the wires without (almost) any help from friction.

A non-self-locking socket is a false socket. As wire ropes are usually operated with a significant safety factor (about 5), even a false socket will be able to provide a good service. However, the wires which are supporting the fluctuation of the line pull are then subject to fatigue.

The socket is unsafe.

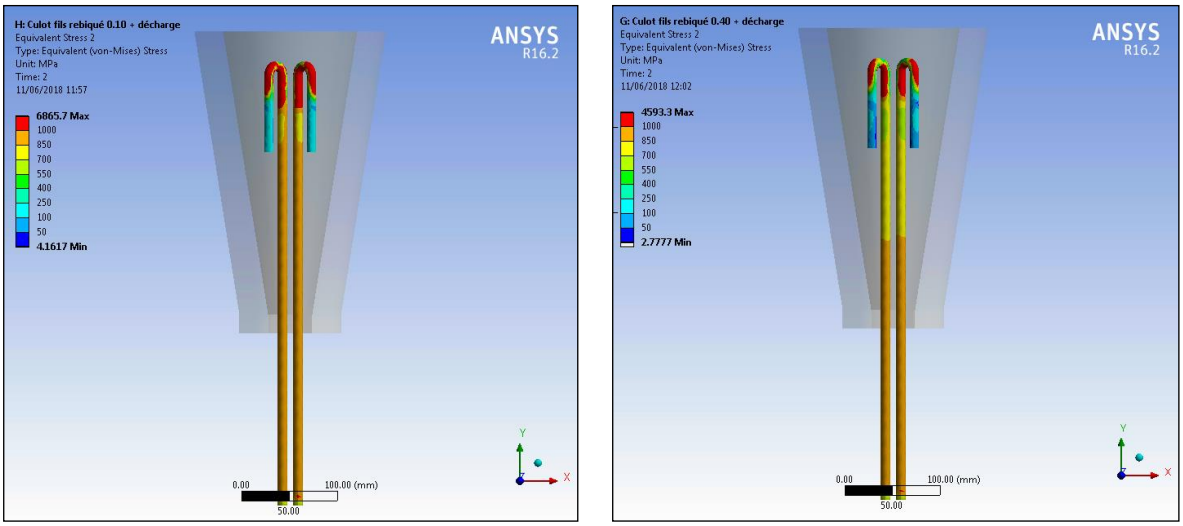

(a) μ = 0.1 (b) μ = 0.4

Figure 33: Transfer of loading along the wires (for different coefficients of friction) in a non-self-locking socket.

Figure 34 below shows the share of the load supported by the hook (continuous line) and by the straight part of the wire, thus by friction (dotted line).

The load is mostly supported by the hook which is located on the top part of the wire.

If the friction coefficient increases, the poured cone which is driven by the hooks is pushed against the socket's body. The resulting pressure makes the wire able to share a part of the load.

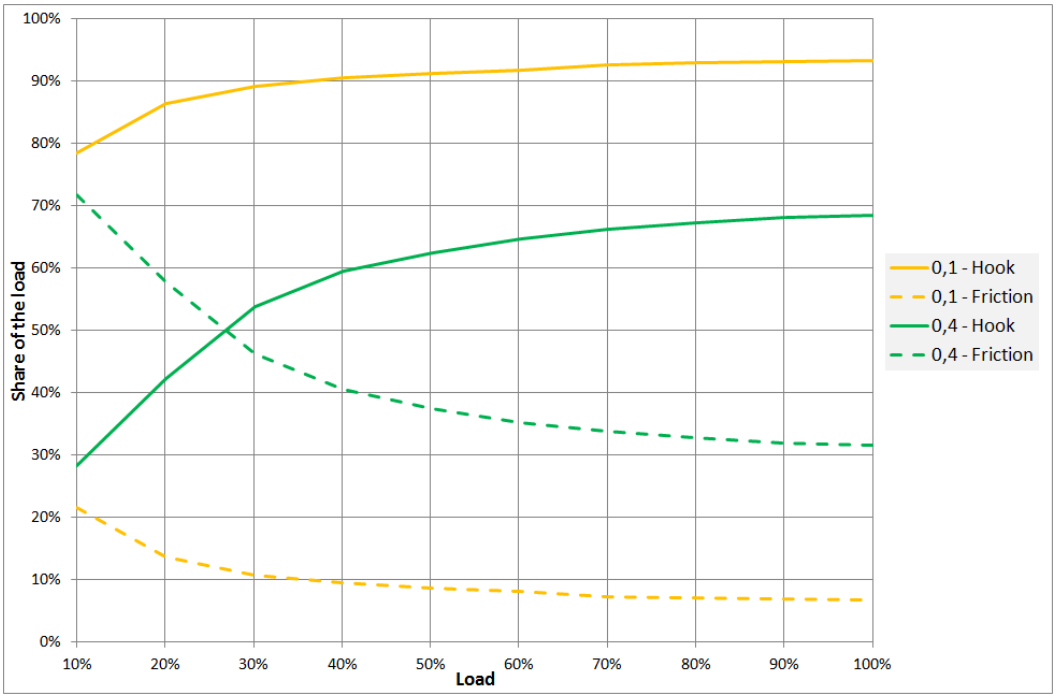

Figure 34: Load sharing in a non-self-locking socket with hooked wires for values of μ = 0.1 and 0.4.

If not all the wires are hooked, the load will only be supported by the hooked wires. Figure 35 presents the results of a simulation with two hooked wires and two straight wires for friction coefficients of 0.1 and 0.4 (non-self-locking configurations). The image in Figure 35 is for friction coefficient μ = 0.1.

The table in Figure 35 shows that if the friction coefficient is 0.4 owing to the pressure applied onto the cone by the hooked wires (see comments above), the straight wires can support a small part of the load.

The socket is really unsafe.

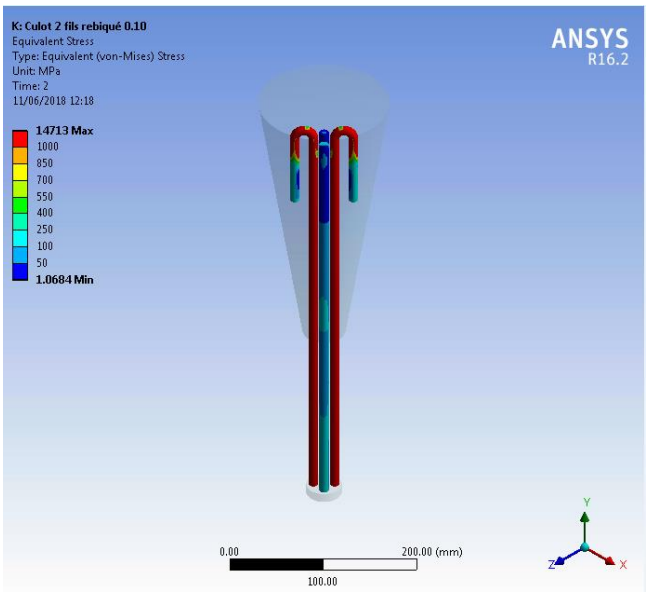

Friction coefficient	Hooked wires	Straight wires
0,10	94,37%	5,63%
0,40	72,67%	27,33%

Figure 35: Socket in non-self -locking configuration with two hooked and two straight wires, μ = 0.1.

7.2 Cone motion restraint

The self-locking behavior can be implemented only if the cone is free to move forward. Any restraint to the motion of the cone will prevent the system from self-locking, even if the friction conditions for the self-locking behavior are fulfilled.

The square cone is a typical example of a false socket. This type of socket may seem attractive as it is easy to fabricate from flat plate. However, if the hole in the bottom plate has a round shape, there are four end stops for the cone motion, at each angle of the base of the cone (Figure 36).

The poured cone, pushed by the hooked wires is extruded from the bottom plate, and the top part of the cone gets dissociated from the rest of the cone…

On a tensile test bed, the socket proved to be able to support the breaking strength of the rope, but what about fatigue…

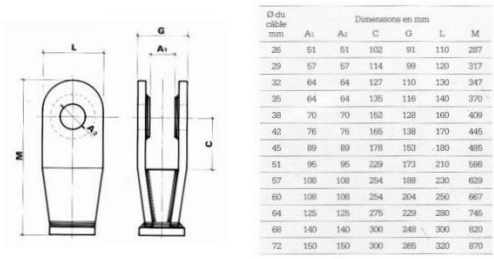

Ø du câble mm	Dimensions en mm					
	A1	A2	C	G	L	M
26	51	51	102	91	110	287
29	57	57	114	99	120	317
32	64	64	127	110	130	347
35	64	64	135	116	140	370
38	70	70	152	128	160	409
42	76	76	165	138	170	445
45	89	89	178	153	180	485
51	95	95	229	173	210	586
57	108	108	254	188	230	629
60	108	108	254	204	250	667
64	125	125	275	229	280	745
68	140	140	300	248	300	820
72	150	150	300	265	320	870

(a) square cone sockets

(b) internal view showing the cone “end stops”

(c) top part of the cone pulls away

(d) extruded bottom

(e) breaking load test

Figure 36: The square cone – an example of a false socket.

Another feature which can prevent self-locking is a groove modifying a proper conical socket (Figure 37). Grooves were introduced as a means to prevent the cone from “popping” out of the back of the socket should it become unloaded, however, they can have the undesired effect of preventing cone slip and initiation of self-locking.

In practice small grooves will not restrain the cone motion as the ring of cast material will just shear off. Larger grooves in sockets should be filled with a suitable material before casting the cone so that a proper cone shape is maintained.

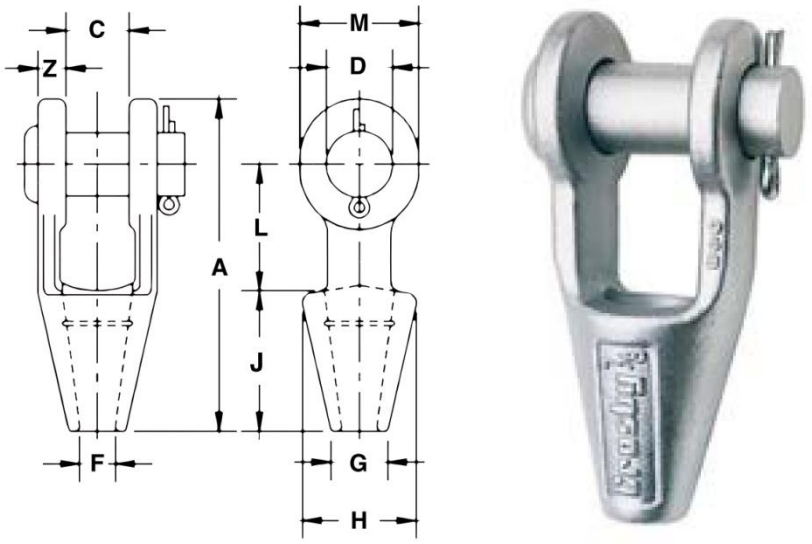

Figure 37: Conical socket basket with groove (from [10]).

8 Real conical sockets

Forces are transferred by friction, thanks to the self-locking configuration. The more the line pull increases, the greater the locking is. This is a DUFOUR socket

The following simulations consider hooked wires in order to make comparisons with the previous section, but the real socket works even with only straight wires.

For a self-locking system, the forces are transferred by friction. Figure 38 presents the results of calculations corresponding to a configuration where the self-locking status was requiring a friction coefficient of 0.65 if we consider the hook and of 0.8 if not.

We can notice that for friction coefficient of 0.80 (clearly self-locking status), the stress in the wire is decreasing as soon as the wire enters the conical zone of the cone.

If this coefficient reduces (0.65) some stresses are visible in the hook area. The termination needs the hook to hold the rope. The termination is no longer working properly.

Figure 39 shows the load supported by the hook (continuous line) and by friction on the straight part of the wire (dotted line).

For the friction coefficient of 0.8 it can be seen that the share of the load supported by the hook reduces when the line pull increases.

For the friction coefficient of 0.65 (which is the threshold for the self-locking condition), for loads up to 40% the force in the wire (friction) is increasing, and above 40% the force decreases.

This confirms that the system was not in a clear self-locking status, and was in fact dependent of the hooks. This example highlights how the hooks can be misleading.

If the self-locking status is clearly reached (friction coefficient of 0.8), even if not all the wires are hooked, the load is however properly distributed among all the wires, Figure 40.

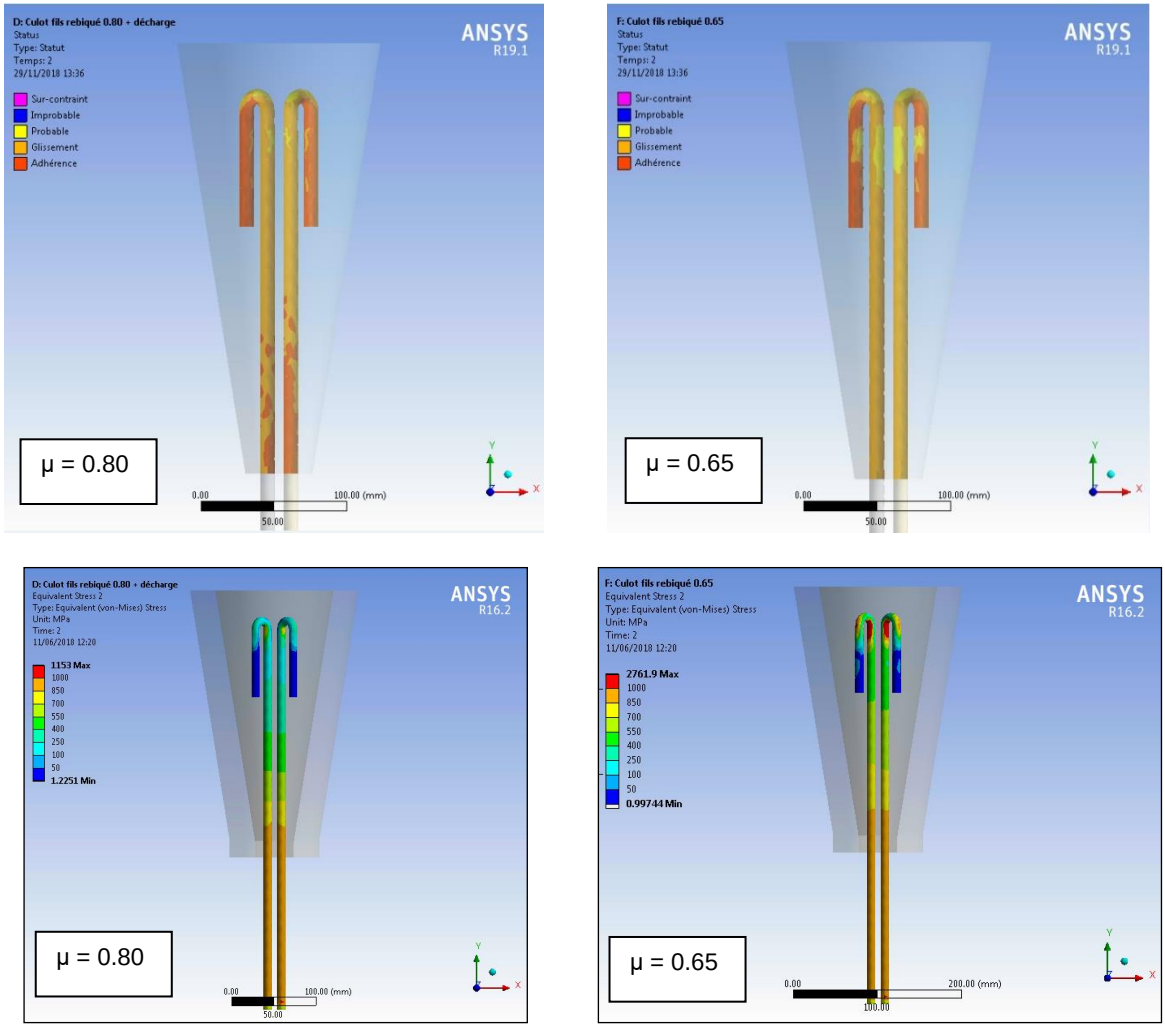

Figure 38: Comparison of the self-locking status of a socket with coefficient of friction μ = 0.8 and 0.65. At the lower value of coefficient of friction it may be seen that there are stresses in the hook rather than transfer of load by friction – the socket is not working correctly.

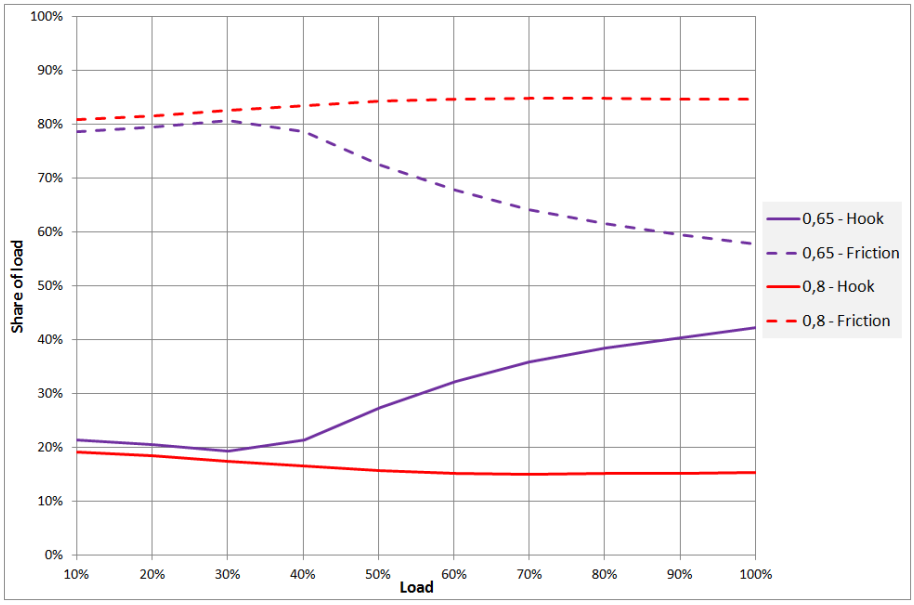

Figure 39: Load sharing in a self-locking socket with hooked wires for values of μ = 0.65 and 0.8.

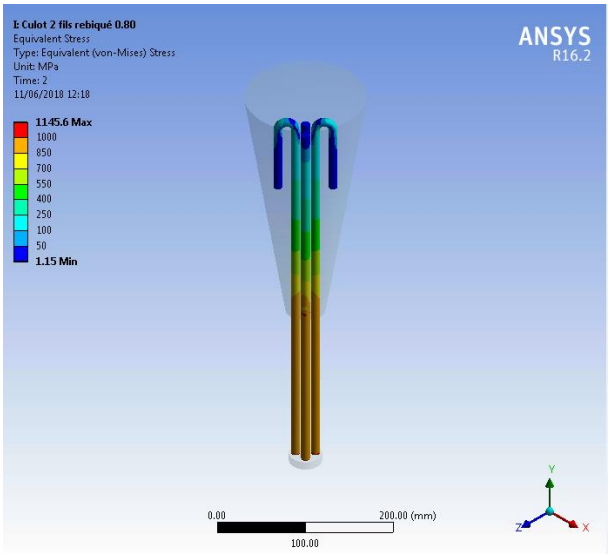

Friction coefficient	Hooked wires	Straight wires
0,65	50,16%	49,84%
0,80	49,96%	50,04%

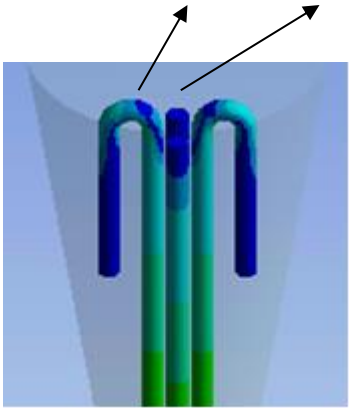

Figure 40: With self-locking status achieved, the loads in the hooked wires and the un-hooked wires are evenly shared.

8.1 Functioning of a real conical socket

The overall compressing force of the wire(s) results from the pressure inside the cone.

This force is calculated as follows:

N = pressure × surface of contact.

Or N = pressure × perimeter × length

Defining:

- n: number of wires
- R_i: radius
- S_i: Section
- P_i: Perimeter
- Perimeter 1 = P_1
- Perimeter 2 = P_2
- φ_1 friction coefficient between the single equivalent wire and the poured cone
- φ_2 friction coefficient between the multiple wires and the poured cone

The force resulting from the friction between the wire and the cone is calculated as follows:

$T = N \cdot tg\varphi_1$ = line pull in the equivalent central wire

$tg\varphi_1$ = T/(pressure × perimeter1 × length)

If we consider a model with “n” wires, providing the same metallic area as the equivalent central wire, the friction coefficient which will provide the same line pull (T) is:

$tg\varphi_2$ = T/(pressure × perimeter2 × length)

$$S_1 = \pi {R_1}^2 \qquad S_2 = n\,\pi {R_2}^2$$

$$P_1 = 2\pi R_1 \qquad P_2 = n\,2\pi R_2$$

$$\frac{P_2}{P_1} = \frac{n\,2\pi R_2}{2\pi R_1} = \frac{n R_2}{R_1}$$

$$S_1 = S_2$$

$$\pi {R_1}^2 = n\,\pi {R_2}^2$$

$$\frac{R_2}{R_1} = \sqrt{\frac{1}{n}}$$

$$\frac{P_2}{P_1} = \sqrt{n}$$

Finally: $tg\varphi_2 = tg\varphi_1/(n^{0.5})$

8.2 Increased number of wires

The limit conditions and forces are the same for all models. Three models are compared, with 1, 4 and 16 wires.

There are the same conditions for the 3 models:

- 9° poured cone
- 15% of diameter rope for thickness of resin
- 0.1 friction coefficient between poured cone and socket
- 0.5 friction coefficient between poured cone and rope

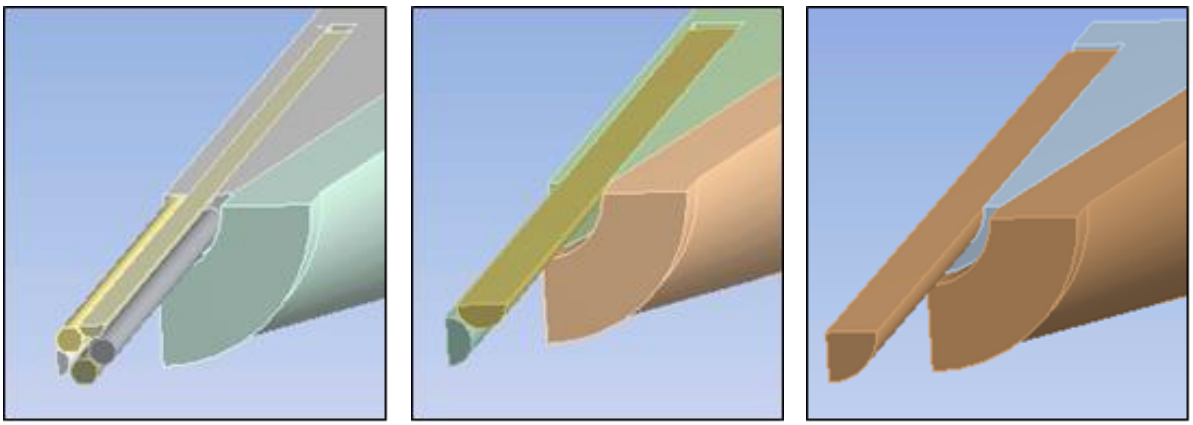

(a) sixteen wires (b) four wires (c) one wire

Figure 41: Model with 16, 4 and one wire.

It can be seen that with the same conditions the 16 wire model has more adherence than the other two.

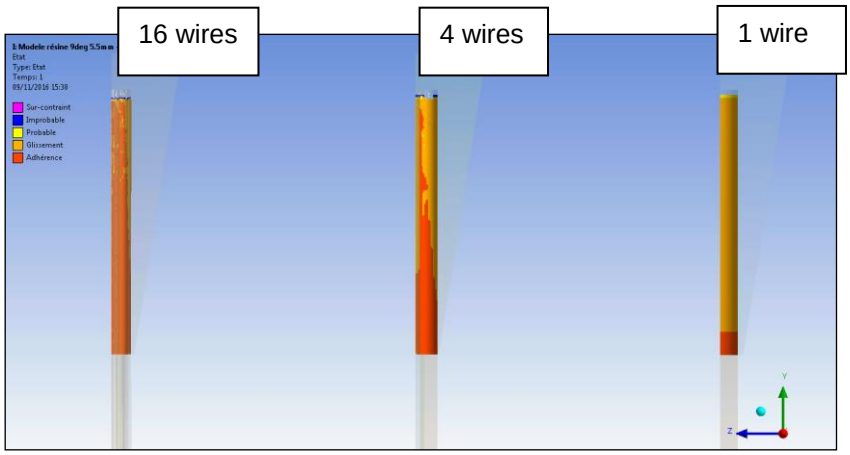

Figure 42: Adherence conditions of the 16, 4 and one wire ropes.

After many models to determine the friction coefficient for each model (1, 4, 12 and 16 wires), the theoretical formula has been validated.

In Table 3 “Calculation” corresponds to the result of the simulation, calculations were performed with several friction coefficients until sliding occurred (status not red).

The cell “Theoretical” corresponds to $0.43/(n)^{0.5}$, where n is the number of wires.

The friction coefficient of the theoretical one wire model can be divided by the square root of number of wires to obtain the real necessary friction coefficient.

Wire number	1	4	9	12	16	50	100
Calculation	0,43	0,23		0,14	0,11		
Theoretical	0,43	0,22	0,14	0,12	0,11	0,06	0,04

Table 3: Comparison of the computer model (calculation) and theoretical results for wire numbers from 1 to 100.

9 Classical conical socket – summary

Summarizing the results of the discussion and analysis thus far:

The classical conical socket relies on the friction between its main components; the socket body, the poured cone, and the wire/fibre.

The real conical socket works as a self-locking mechanism, the greater the line pull increases, the more the restraining force increases.

Parameters influencing the functioning of a socket have been investigated with the following key findings:

- The poured cone must remain free to move.
- Any movement restrainer must be avoided (§7.2).
- The system needs an initiation system (§5.2).
- The hooking of some wires can be a solution.

- But hooking wires can be misleading (§8).

The friction coefficient between the wires and the poured material is about the same as the coefficient between the socket body and the poured material. Because of the roughness of the “standard” socket body it could even be smaller.

Thus the socket can work only thanks to the number of wires (§8.3).

Getting the self-locking configuration with a small number of wires requires a very high friction coefficient, and therefore this is almost impossible.

When all the wires are hooked, the system will be able to transfer the line pull in the rope even if the self-locking conditions are not fulfilled (false conical socket - § 8.1). However, this condition should be avoided as only the hooks will be loaded, there will be a stress concentration which will lead to very poor fatigue behavior.

10 Hybrid rope socket – a new concept

Thus far, this paper has described how a proper and safe socket termination must work as a self-locking mechanism. The self-locking behavior of the system mainly depends on the geometry of the parts, and on the friction coefficient between these parts.

The analysis has shown how for a classical conical socket these parameters are interdependent, thus optimizing one parameter can lead to a worsening of the situation for other parameters. For example reducing the cone angle in order to make the system working with a smaller friction coefficient generates a higher pressure on the rope, and then the termination fails because of an overloading of the rope.

The new hybrid socket described in this paper makes possible to split the functions, and thus to optimize each of the functions without this impacting on the other.

- Function 1: creation of the bearing pressure.
- Function 2: management of this pressure.

The creation of the bearing pressure is performed thanks to wedges. The friction coefficient between the wedge and the socket body must be as small as possible. Thus this interface is machined with accuracy, and can be lubricated.

The friction coefficient between the wedge and the rope must be as big as possible. Thus teeth are machined on the face of the wedge in contact with the rope. The contact between the wedge and the rope will be not only friction but also with mechanical closure.

The management of the bearing pressure is performed by means of a resin sleeve. Increasing the thickness of this sleeve makes it possible to reduce the bearing pressure and thus to reduce the stresses onto the rope.

An additional benefit is that the termination is dismountable and re-usable. The same sleeve can be re-installed several times (e.g. for installation of the rope through the sheaves of a multipart reeving system, or to permit the inspection of the rope which is located inside the connector).

11 A new hybrid socket®

Figure 43 shows a section view of the new termination [11]. The forces are transferred by friction owing to the self-locking configuration. The wedges are part of the mechanical elements. They are accurately machined, and as mentioned above, the contact between the wedge and the socket body can be lubricated/greased.

The poured material consists of a cylindrical sleeve formed around the rope (this sleeve is critical and needs to be manufactured correctly and with appropriate materials).

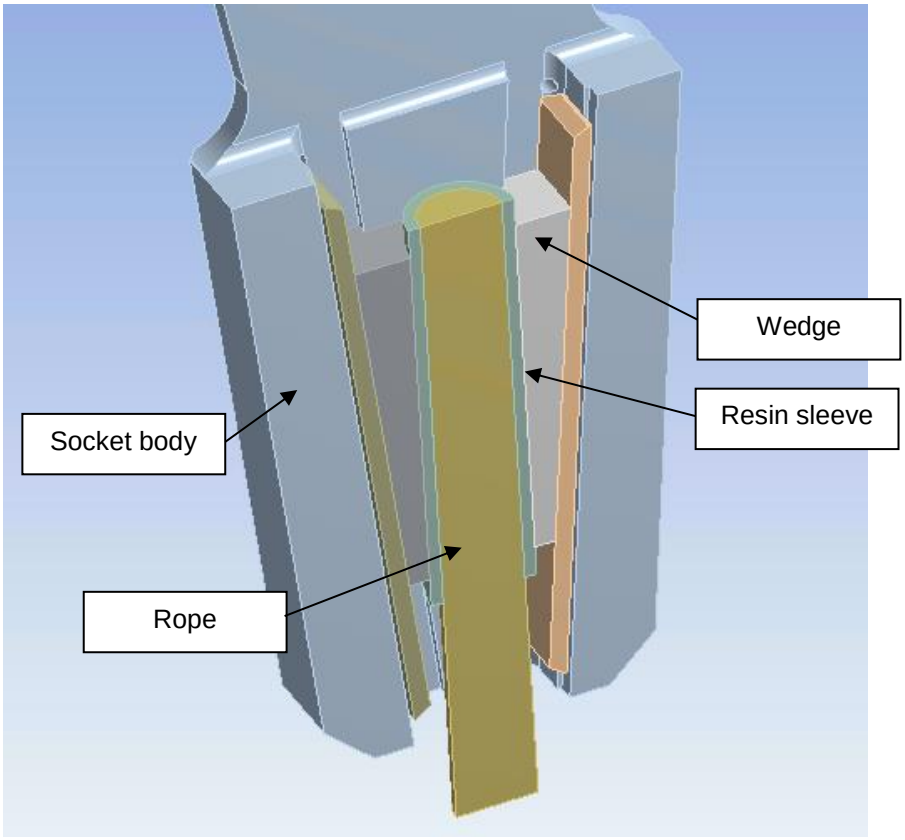

Figure 43: Section view on the hybrid socket®.

The termination may be formed without a resin sleeve for wire ropes. However, for fibre ropes, the sleeve is obligatory.

Since the resin sleeve is a cylinder the shrinkage along the length is linear. The bearing pressure will be almost uniformly distributed along the length of the rope elements.

Figure 44 shows examples of a resin sleeve on wire and fibre ropes. The sleeved end of the rope is introduced into the termination through the lower end, and then locked into place as it is pulled forward.

The wedges may either be pulled in by the rope as it is loaded, or, as discussed later may be “externally locked” by pressing forward from behind. In either case, the contact between the wedges and the resin sleeve generates imprints in the sleeve (Figure 45), there is a kind of mechanical closer which secures the self-locking behavior of the system.

Figure 44: Wire (top) and fibre (bottom) ropes with cylindrical resin sleeve ready for mounting the in wedge socket.

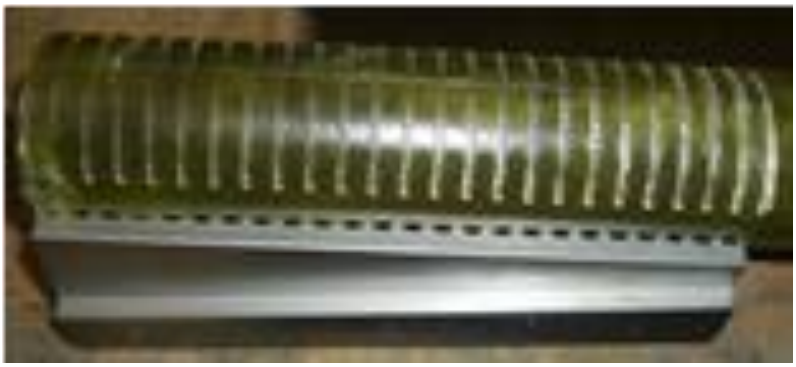

Figure 45: Imprints on the resin sleeve from the wedge faces after loading in the socket.

Now the forces have to be transferred from the sleeve to the strands/wires/fibres of the rope.

Here there are two opposing parameters which influence the diameter of the resin sleeve:

- Reducing the sleeve's diameter will increase the friction capability, but also increase the stresses onto the rope and will possibly lead to the failure of the termination in the wedges zone.
- Increasing the sleeve's diameter will reduce the stresses onto the rope but will also reduce the friction capability, and then the termination may fail because of the sliding of the rope inside the sleeve.

As for the classical conical socket, the transfer will require a very high friction coefficient if the number of wires/strands is very low. For a (1+6) construction the system works only with non-compacted strands because the "friction coefficient" is increased, thanks to the roughness of the strand.

Once the number of wires/strands is fifteen or more, we can determine an optimum sleeve diameter.

In the case of a fibre rope, once the sleeve if poured, the system behaves exactly the same as with a wire rope.

The transmission of the force to the fibres (internal part of the rope) is even easier than with a wire rope, since, owing to the huge number of fibres, the friction coefficient between the resin and the fibre can be very low.

Thus for a fibre rope the outer diameter of the sleeve can be defined only on the basis of the pressure which will be optimal for the fibres.

12 Initial test results

Initial tests were undertaken by DEP on small ropes of typically Ø10 – Ø12 mm. Subsequently tests were undertaken by DEP and TTI on ropes up to Ø16 mm. Over 150 tests have been performed to date. This section presents a summary of the key findings.

12.1 Wire ropes

12.1.1 Wire ropes without resin sleeve

Over sixty tests have been conducted to date on rope diameters Ø7 – Ø16 mm. These cover a wide variety of constructions including:

- 19×7
- 7×19
- Spiral strand (1+6)
- Veropro 8 (an 8 strand rope with IWRC and intermediate plastic layer)
- Veropower 8 (an 8 strand rope swaged construction with intermediate plastic layer)
- Verotop (die-formed 35 strand (1+K6+K6/K6+16) rotation resistant)

The following parameters have been investigated:

- length of the wedge (4×d, 6×d, 10×d)
- type of locking; natural (self-locking), external,
- type of loading; straight tensile pull, cycled (tension fatigue)
- removal of the internal plastic layer

For the wire ropes without a resin sleeve, the ropes systematically broke inside the socket at the edge of the wedge. The static breaking strength varied over the range 85% to 100% of the MBL of the rope.

At time of writing this paper, only wire ropes without a resin sleeve have been tested in fatigue. Figure 46 shows the results for a series of tests conducted on a Verotop rope. These tests were all conducted with 6×d wedges (apart from the test conducted with resin cones which was undertaken for comparison).

Four variants may be seen:

- Self-locking – no pre-pull: the sleeve was positioned in the wedges in the socket. The setting of the wedges was provided by the first loading to the peak load of the cyclic loading.
- Self-locking – pre-pull: the sleeve was positioned in the wedges and an initial load of +15% of the peak load of the cyclic loading was applied to set the wedges before the fatigue cycling commenced.

- External locking: the sleeve was positioned in the wedges and an external load of +15% of the peak load of the cyclic loading was applied to the back of the wedges to set them before the fatigue cycling commenced.
- Conical sockets: resin conical socket at each end with initial +15% of the peak load applied before fatigue cycling commenced (to permit comparison with the other results).

The self-locking samples all show a step change in the maximum machine stroke in the early part of the test. This is thought to be associated with the wedges slipping forward, and exacerbated by an attendant overload as the machine controller increase the machine gain to achieve the required load (and overshoots).

The results show that the self-locking – no pre-pull and external locking have a similar endurance. The self-locking – pre-pull 100kN and the conical socket sample both have improved performances, which are due in part to the initial overload of the sample. The wedge socket has an endurance approximately up to 80% of the conventional conical socket sample.

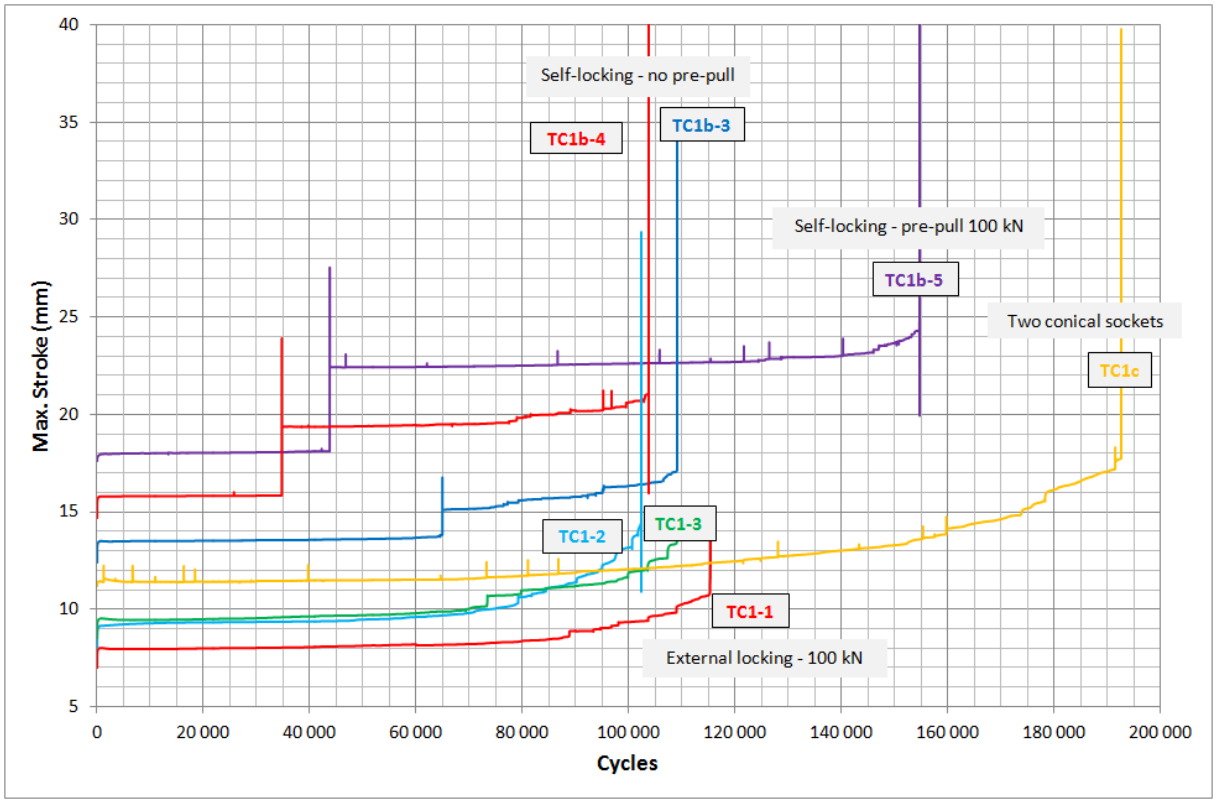

Figure 46: Maximum stroke as a function of cycles for Verotop samples with no resin sleeve (different initial wedge setting conditions) and for comparison a standard sample with resin conical sockets.

12.1.2 Wire ropes with a resin sleeve

Over forty-five tests have been conducted on ropes with diameters Ø7 – Ø16 mm fitted with a resin sleeve. As with the “bare” ropes, these cover a wide variety of constructions including:

- 19×7
- 7×19
- Spiral strand (1+6)

- Veropro 8 (an 8 strand rope with IWRC and intermediate plastic layer)
- Veropower 8 (an 8 strand rope swaged construction with intermediate plastic layer)
- Verotop (die-formed 35 strand (1+K6+K6/K6+16) rotation resistant)
- Eurolift

The test results showed that almost without exception the rope does not break in the connectors, Figures 47 and 48, (except the spiral strand 1+6 of 7 mm, which is to be expected because of the small number of wires, there was slippage of the rope with a sleeve of 16 mm and break inside the connector with a sleeve of 12 mm. This breaking strength was almost the same (61 kN compared to 58 kN) as for a test without resin sleeve).

It is emphasized that the two tests which failed for this rope construction (1+6) confirms the calculation results and indicates that such rope construction is probably not suitable for any socket termination

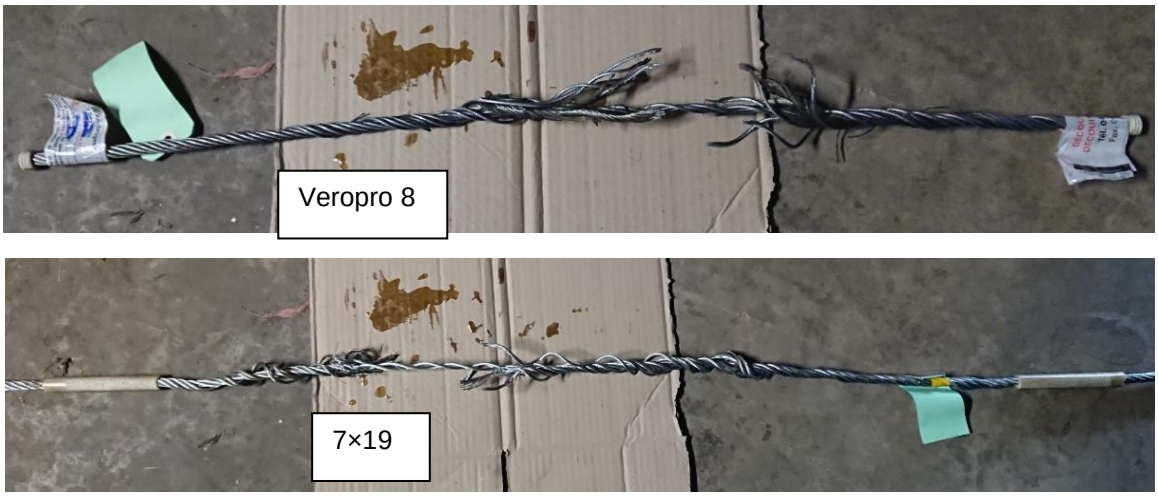

Figure 47: Showing samples of Veropro 8 and 7×19 construction terminated with resin sleeves after tensile testing. Failure was well clear of the end fittings.

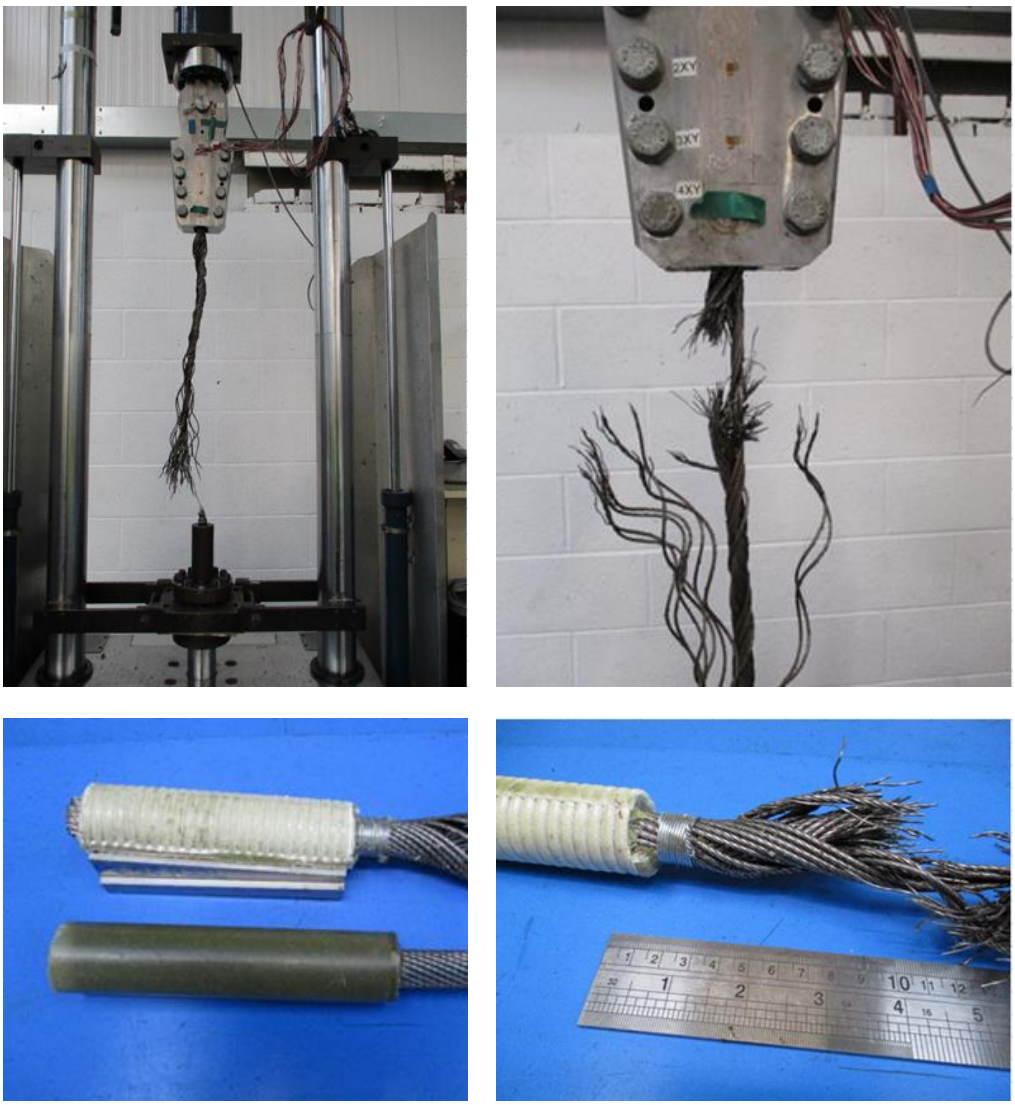

Figure 48: Showing samples of Verotop wire rope construction terminated with resin sleeves after tensile testing to failure. Failure location was clear of the wedge fittings.

12.2 Fibre ropes

12.2.1 HMPE

To date 37 tests have been performed on a variety of different rope constructions manufactured by Cousin Trestec (France), OTS (Norway), Samson (USA) and Yale Cordage (USA). The rope diameters were all in the range Ø6 mm to Ø11 mm.

Figure 49 shows a typical example of a HMPE rope test: the rope does not break in the connector.

Figure 49: Example of HMPE rope breaking load test showing failure in the free length of the sample (Ø11 mm, ULTREX, Yale Cordage).

12.2.2 Aramid

A total of eight tests have been performed on ropes from Cousin Trestec (France) and Yale Cordage (USA). The rope diameters were all in the range Ø6 mm to Ø11.4 mm. As with the HMPE ropes, the samples do not break in the connector (Figure 50).

Figure 50: Example of aramid rope breaking load test showing failure in the free length of the sample (Ø11.4 mm, Tech-Kern, Yale Cordage).

12.2.3 LCP

Only three tests have been performed on LCP ropes from Yale Cordage (USA). The rope diameters were in the range Ø8 mm to Ø10 mm. As with the other fibre rope materials, the samples did not break in the connector (Figure 51).

Figure 51: Example of LCP rope breaking load test showing failure in the free length of the sample (Ø10 mm, Vectrus, Yale Cordage).

13 Conclusions

This paper has presented the results of an in depth finite element analysis for a self-locking conical socket. The results have shown the importance of friction between the main components, importantly that between the poured cone and the wire/fibre. A true conical socket operates as a self-locking mechanism, the greater the line pull increases, the more the restraining force increases.

Various parameters which influence the functioning of a socket have been investigated with the following key findings:

- The poured cone must remain free to move, and any movement restrainer must be avoided.
- The conical socket needs an initiation system.
- The hooking of some wires can be a solution, but hooking wires can also be misleading.

The friction coefficient between the wires and the poured material is about the same as the coefficient between the socket body and the poured material. Because of the roughness of the “standard” socket body it may even be smaller. Consequently, the socket only works thanks to the number of wires/fibres.

Obtaining the self-locking configuration with a small number of wires/fibres requires a very high friction coefficient, which is almost impossible to achieve.

When all the wires are hooked, the system will be able to transfer the line pull in the rope even if the self-locking conditions are not fulfilled (false conical socket). However, this condition should be avoided as only the hooks will be loaded, there will be a stress concentration which will lead to very poor fatigue behavior.

A new Hybrid Socket® has been presented, the design of which builds on the findings from the analysis of the conventional self-locking socket. In this new design the functions of *creation* and *management* of the bearing pressure are separated, meaning that the two may be independently optimized.

Initial breaking load tests undertaken on wire ropes without the resin sleeve showed that the new design hybrid socket could achieve 85% - 100% of the rope MBL. Samples failed at the end of the wedge grips, as might be expected. In fatigue tests, the samples also broke at the sockets. In a comparative test with a sample with resin socket terminations the sample achieved up to 80% of the endurance of the "conventional" socket.

The breaking load tests on wire and fibre ropes with resin sleeves are very encouraging: the wire and fibre rope samples failed clear of the terminations. (It is noted that some tests were made exploring the effect of varying the thickness of the resin sleeve, and that some of these samples failed in the termination, as expected.) At time of writing the fatigue tests with the resin sleeves are about to commence.

14 Acknowledgements

The authors wish to acknowledge and thank the following for their contribution to this work:

- Mathieu Fournier who built the numerical model and carried out all the calculations
- Thierry Leroux who was in charge of all the tests at DEP, and who was assisted by Alberto Debarros.
- Robert Carr, who prepared the resin conical sockets on the wire rope samples tested at TTI Testing and set up all the tests.
- Verope, Yale Cordage and Millfield Manufacturing for providing the ropes and resin materials used in this work.

Finally thanks are due to Millfield Terminations for permitting publication of this study.

15 References

[1] **Ridge, I.M.L. and Verreet, R.** Wire rope end connections: an overview. OIPEEC Round Table Conference "Rope Terminations and Fittings", Bethlehem USA August 20th-22nd 2001 1-29 ISBN: 0 7049 2284 1.

[2] **McKenna, H.A., Hearle, J.W.S. and O'Hear, N.** Handbook of fibre rope technology, Woodhead Publishing Ltd, Cambridge, UK, 2004, ISBN 1 85573 606 3.

[3] Analyse et extrait des deux ouvrages de Mr Guillaume Henri Dufour sur les ponts suspendus. Annales des Ponts et Chaussées – 1832.

[4] **Blackett, W.C.** A Method of Socketing a Winding-Rope, and its Attachment to a Cage Without the Use of Ordinary Chains, Trans IMinE, 1901-1902, Vol XXIII, pp 10-16.

[5] **Dodd, J.M.** Resin as a Socketing Medium, *Wire Industry*, May 1981, pp 343-344.

[6] **Corden, C.H.H.** The Development of Resin Cappings for Wire Ropes in Mines, Part 1: The History of the Development of Resin Cappings in the UK, *Mining Technology*, Vol 77, No 883, March 1995, pp 90-96.

[7] **Flory, J.F.** Improved potted socket terminations for high-modulus synthetic-fibre rope, Proc. OIPEEC Round Table Conference "Rope terminations and

fittings", Bethlehem, USA, August 20th-22nd 2001, 125-136 ISBN: 0 7049 2284 1.

[8] **Bradon, J.E., Chaplin, C.R. and Ridge, I.M.L.** *Analysis of a resin socket termination for a wire rope.* J. Strain Analysis **36**(2001)1 71-88.

[9] **Bradon, J.E. and Ridge, I.M.L.** *Comparison of white metal and resin socket terminations for wire ropes.* J. Strain Analysis **38**(2003)2 149-160.

[10] **Crosby**, Manufacturer's General Catalogue, 2016 Metric, Published by The Crosby Group LLC, Tulsa, OK 74110, USA.

[11] Invented by **Jean Marc TEISSIER**. United Kingdom Patent Application N° 1821015.3 by Millfield Terminations Ltd.